

AD-A047 773

AIR FORCE INST OF TECH WRIGHT-PATTERSON AFB OHIO SCH--ETC F/G 20/6
DESIGN AND EVALUATION OF COUPLERS FOR A MULTIMODE SINGLE FIBER --ETC(U)
OCT 77 M C OGAN

AFIT/GE0/PH/77-2

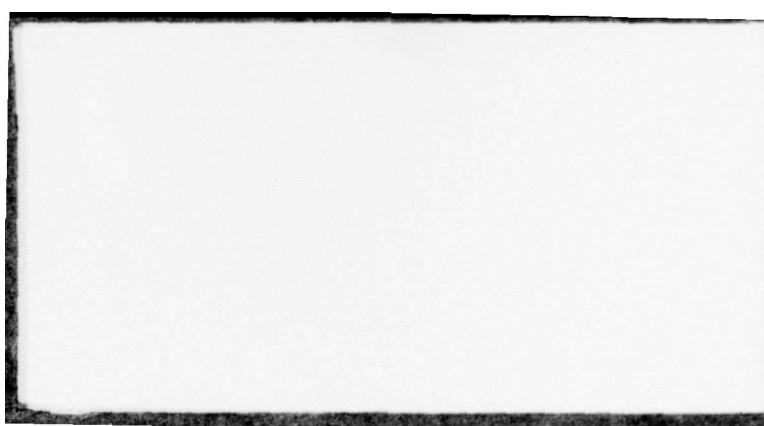
NL

UNCLASSIFIED

| OF |
AD
A047 773



END
DATE
FILMED
| 78
DDC



GEO/PH/77-2

1

DDC
RECEIVED
DEC 19 1977
F

DESIGN AND EVALUATION OF COUPLERS
FOR A MULTIMODE SINGLE FIBER
OPTICAL DATA BUS

THESIS

GEO/PH/77-2

Michael C. Ogan
2nd Lt USAF

Approved for public release; distribution unlimited

14 AFIT/
GEO/PH/77-2

6 DESIGN AND EVALUATION OF COUPLERS
FOR A MULTIMODE SINGLE FIBER
OPTICAL DATA BUS.

9 Master's THESIS,

Presented to the Faculty of the School of Engineering
of the Air Force Institute of Technology
Air University
in Partial Fulfillment of the
Requirements for the Degree of
Master of Science

by
10 Michael C. Ogan B.S.
2nd Lt USAF
Graduate Electro Optics

11 October 1977

12 85p.

Approved for public release; distribution unlimited.

1473
012 225

4B


Preface

This thesis is primarily an experimental one and for the most part, limited to a specific area of fiber optics. While it is assumed that the reader is familiar with optics and electrical engineering, a brief overview of optical fibers and the relation of couplers to fiber optics in general is presented.

Many thanks are due to Elgene R. Nichols, my Lab Advisor and sponser of this thesis, whose guidance and aid were invaluable. Thanks must also go to my Faculty Advisor, Dr. B. Kaplan, who contributed greatly toward my understanding through critical appraisal of this thesis. I am grateful to many people at the Air Force Avionics Laboratory/DHO, most notably Mr. W. Borodatschew, whose glass working abilities were essential in the fabrication of several couplers.

The contribution of the many authors cited in the bibliography must be acknowledged. Any errors or misconceptions found in this thesis are due to my ignorance in interpreting their work.

I would like to personally thank my wife, Debbie, for typing this thesis.

ACCESSION for	
NTIS	Wife Section <input checked="" type="checkbox"/>
DDC	Self Section <input type="checkbox"/>
UNCLASSIFIED	<input type="checkbox"/>
DISTRIBUTION	
BY	
DISTRIBUTION/AVAILABILITY CODES	
SPECIAL	
	

Contents

	Page
Preface.....	ii
List of Figures.....	iv
List of Tables.....	vi
Abstract.....	vii
I. Introduction.....	1
II. Theory.....	5
Energy Propagation in a Waveguide.....	5
Coupler Design.....	15
III. Experimental.....	24
Equipment and Set-up.....	24
Hughes Tee Coupler Evaluation.....	27
Spectronics Star Coupler Evaluation.....	33
Experimentally Fabricated Couplers.....	35
a) Directional Couplers (DC-1, DC-2).....	37
b) Tee Coupler (TC-1).....	42
c) Star Couplers (SC-1, SC-2, SC-3).....	43
d) Star Coupler (SC-4).....	51
e) Star Couplers (SC-5, SC-6).....	58
ITT Fused Star Coupler Evaluation.....	61
IV. Summary, Conclusion and Recommendation.....	65
Bibliography.....	68
Appendix: Detector Linearity Measurement.....	70

List of Figures

<u>Figure</u>	<u>Page</u>
1. Representation of slab waveguide with perfectly conducting mirror surfaces.....	6
2. Schematic of clad optical fiber.....	11
3. Ray tracing at the core-cladding interface.....	12
4. Schematic of frustrated total reflection prism-thin film coupler.....	16
5. Schematic of mixing rod design consideration.....	17
6. Directional and tee couplers using mixing rod.....	19
7. Star coupler design (4-port).....	19
8. Diagram of EM wave incident on boundary between two dielectric media (Ref 5:38).....	21
9. Set-up for fiber dimension measurement.....	25
10. Experimental set-up for coupler efficiency measurement.....	26
11. Schematic of Hughes single fiber fused tee coupler.....	28
12. Internal reflections in coupled fiber.....	31
13. Eight-port star coupler.....	33
14. Star coupler placement in test apparatus.....	34
15. Experimental measurement of NA_f	38
16. Schematic of DC-1.....	39
17. Output side of DC-1.....	40
18. Output side of DC-2.....	40
19. DC-1 in experimental set-up.....	40
20. Schematic of TC-1.....	43
21. General design of star coupler using cement-filled mixing rod.....	44
22. Diagram of index measuring set-up.....	45

<u>Figure</u>	<u>Page</u>
23. Diagram of star coupler with solid mixing rod.....	52
24. Microscopic photograph of mixing rod for SC-4.....	53
25. Schematic of fused fiber star coupler.....	58
26. Photograph of SC-5: ITT fibers.....	60
27. Photograph of SC-6: Corning fibers.....	60
28. Star coupler made from ITT fused fibers.....	61
29. Set-up for detector linearity measurement.....	70
30. Plot of detector voltage vs. power received.....	72

List of Tables

<u>Table</u>	<u>Page</u>
I. Data taken from Hughes Tee Coupler HTC-32.....	30
II. Data taken from Spectronics Star Coupler.....	36
III. Data from Directional Coupler DC-1.....	41
IV. Data from Star Coupler SC-3.....	47
V. Data from Star Coupler SC-4.....	54
VI. Data from ITT Fused Fiber Star Coupler.....	62
VII. Comparison between Star Couplers.....	66
VIII. Detector Output for Neutral Density Filters.....	71

Abstract

The fiber optic couplers designed and evaluated in this thesis are intended primarily for use in aircraft avionics systems, and consist of single strand, multimode fibers with step index profiles. Types of couplers considered are the directional, tee, and star couplers, with emphasis on the latter. Several designs are fabricated and tested, including three kinds of star couplers. The first employed a mixing rod of transparent cement and yielded an average transmission factor of 0.009 (-20.5 dB), with an average insertion loss of -12.83 dB. The second was formed with a solid quartz mixing rod, producing an average transmission factor of 0.003 (-25.2 dB) and an average insertion loss of -18.01 dB. The third star coupler's mixing rod was made by fusing the individual fibers, resulting in an average transmission factor of 0.01 (-20.0 dB) and an average insertion loss of -12.35 dB. After theoretical and experimental comparison between performance efficiencies, the third coupler is recommended as an optimum design for a fiber optic data bus system.

INTRODUCTION

Fiber optics is becoming increasingly important in digital communications and has several important potential advantages over conventional wiring for managing the flow of signals between aircraft avionics systems. These advantages include greater bandwidth, less weight, and freedom from radio frequency and electromagnetic interference. An application of a fiber optic system requires the use of a data bus, or trunk line, which distributes the signal among several terminals. At each terminal, there must be an input/output coupler such that a signal from the data bus may be coupled to the terminal and vice versa. The implementation of a data bus necessitates the development of efficient and durable couplers. Some work has been done in this area, but the realization of an optimum coupler for Air Force needs is yet to be made.

Fiber optic systems can be divided into the following two basic classes: those which employ a single strand of fiber and those which utilize many of these strands in a fiber bundle. Although more study has been done on the latter, indications are such that the single fiber system will become more important.

For instance, fiber bundles have several inherent disadvantages, including lack of fiber-to-fiber registration, packing fraction loss at cable terminations, and relatively high absorption loss. The third factor, that of absorption, contributes significantly to power attenuation as a signal travels along the fiber bundle. Because of the need for many fibers in a bundle system (200 to 300 are common per bundle), economic

manufacture of them results in the use of inexpensive, and therefore lossy, materials. A single fiber system, on the other hand, requires fewer fibers per data link (4 to 7 for redundancy), enabling the use of materials which yield much less attenuation. In addition, the only major disadvantage of a single fiber system is the alignment problem at connecting interfaces.

Single fibers can also be divided into sub-groups. These include single mode and multimode fibers, each of which can have either a step-index or graded-index profile. The distinction between single and multimode fibers will be more clearly understood after the mode analysis is done in the theoretical section. By way of introduction, however, it can be said that single mode fibers are still in the developmental stage, and consist of very small diameters, making splicing and coupling alignment extremely critical. Multimode fibers, on the other hand, are readily available, have a larger diameter (thus they are easier to work with), and have a larger information carrying capacity.

The other classification mentioned is related to the refractive index profile of the fiber. Step index fibers consist of a core made of one index which is surrounded by a cladding of a lower index. Graded index fibers are produced such that the index of refraction changes continuously as a function of the fiber's radius. The graded index was developed to reduce the phenomenon of signal pulse spreading or dispersion in a fiber optic system. As an illustration of dispersion in these two kinds of fibers, Ref 18:31 shows that for a step index

fiber, the dispersion is commonly 15-30ns/km, whereas a graded index fiber yields a dispersion of only 0.17ns/km. This difference would be important for a system which extends for several kilometers. However, the couplers being designed here are primarily intended for use in an avionics system, where the short length of fibers required would render the difference in dispersion negligible. For the reasons mentioned above, then, the fibers used for this project will be limited to the multimode, step index type.

Another consideration involves the kind of coupler to be dealt with. There are three basic types: the directional, the "tee", and the star or radial coupler. The first of these has three ports (fiber ends or terminals) and is used for splitting the incoming signal in two. The "tee" coupler consists of four ports, and can be used to couple into and out of a data bus. The star, or radial coupler has a variable number of ports, and can be centrally located in a system to couple the signal from any single fiber into all the rest. Because of the unique nature of the star coupler (requiring only one coupler for a given system, compared to the "tee", which requires one coupler for every terminal in the system), concentration in this thesis will be centered there.

The specific problem at hand will be concerned with the evaluation of existing couplers, and the design and fabrication of several multimode, single fiber couplers, with emphasis on the star coupler. Since the basic approach to this problem will be an experimental one, the organization of this thesis will consist of a brief theoretical section followed by an

experimental analysis. The theory covered will include a look at the general idea of energy propagation in a waveguide and will address the aspects of coupler design. The experiments described incorporate both the testing of available couplers and the evaluation of certain couplers constructed specifically for this project. The concluding section deals with a comparison between various designs and makes recommendations for an optimum radial coupler.

THEORY

Energy Propagation in a Waveguide

Every fiber optic system consists of the following three basic units: a source, a detector, and a fiber link between them. Any design dealing with the latter, which includes fiber optic couplers, necessitates an understanding of waveguide propagation, since an optical fiber is simply a cylindrical, dielectric waveguide. The first portion of this theoretical section deals with defining a waveguide and analyzing its ability to propagate energy. To do this, the simple model of a slab waveguide with conducting walls is employed, allowing the description of characteristic waves, or waveguide modes. From that point, the discussion is extended to include a dielectric slab waveguide, which describes a more complete set of modes. Finally, a simple model of a clad optical fiber is considered, using geometrical optics.

A waveguide can be defined as "any structure capable of guiding the flow of electromagnetic energy in a direction parallel to its axis, while substantially confining it to a region either within or adjacent to its surfaces (Ref 1:7)." From a physical optics point of view, a description of this energy flow might deal with the superposition of uniform plane waves propagating along the waveguide, while being internally reflected at various angles to its axis. For simple guide structures, an analysis using this idea is possible. However, for a more complicated structure (e.g. one without plane walls), such analysis would be quite difficult (Ref 1:8). For

this reason, it is common to select another set of elementary waves to work with, called modes. A waveguide mode in a general sense is defined as "an electromagnetic wave that propagates along a waveguide with a well-defined phase velocity, group velocity, cross-sectional intensity distribution, and polarization (Ref 1:8)." Modes can be called "characteristic waves" in that they satisfy the homogeneous wave equation in the media of the guide, and also satisfy the boundary conditions at the interfaces. Therefore, a mode is dependent on the structure of the guide rather than the radiation source which excites it. Each mode can be described in terms of the superposition of uniform plane waves propagating at a fixed angle to the axis of the guide.

As a starting point in discussing the propagation of the modes defined above, consider a slab waveguide consisting of two parallel plane mirrors assumed to have perfectly conducting surfaces and be infinite in extent. Let x be the direction perpendicular to the mirrors and z be the assumed direction of propagation (Fig. 1). For simplicity, let the lower

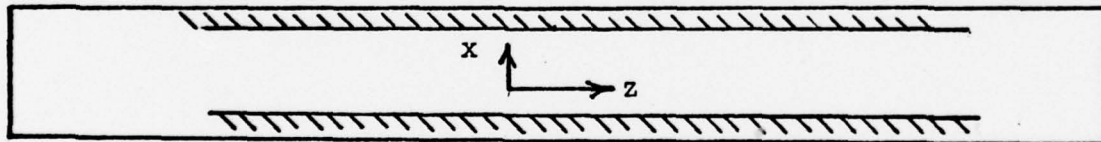


Fig. 1. Representation of slab waveguide with perfectly conducting mirror surfaces

mirror surface be removed and consider a plane wave incident on the upper mirror whose Poynting vector is at an angle θ with respect to the normal to the surface. If the incident wave is assumed to be plane polarized with its electric vector being perpendicular to the plane of incidence, then the elec-

tric vector has only its y-direction component,

$$E_{yi} = E_0 \exp[i\omega t - ikx \cos\theta - ikz \sin\theta] \quad (1)$$

where the subscript i means incident, E_0 is its amplitude, $k = \frac{2\pi n}{\lambda_0}$ is its wave number, λ_0 is the free-space wavelength, and n is the refractive index. To satisfy the boundary condition, the tangential component of the electric field must vanish at the perfect conductor, meaning the reflected component E_{yr} , of the electric vector is

$$E_{yr} = -E_0 \exp[i\omega t + ikx \cos\theta - ikz \sin\theta] \quad (2)$$

The total electric field in the region below the conductor would then be

$$E_y = E \sin(kx \cos\theta) \exp[i\omega t - ikz \sin\theta] \quad (3)$$

which was obtained by combining equations (1) and (2) and using the relation $e^{i\phi} - e^{-i\phi} = 2i \sin\phi$. All constants for simplicity have been absorbed into the complex-valued constant E . Equation (3) can now be seen as the electric field of a non-uniform plane wave traveling in the z direction with a phase velocity $\frac{w}{k \sin\theta}$. Since the electric field is transverse to the assumed direction of propagation, the wave is called a transverse electric (TE) wave. The magnetic field of a TE wave has a component in the z direction, in addition to transverse components.

A common way of writing the total electric field in equation (3) is the following:

$$E_y = E(\sin Bx) \exp[i\omega t - ihz] \quad (4)$$

where h is called the propagation constant or longitudinal wavenumber and B is called the transverse wavenumber. From this, a guide wavelength is defined as $\lambda_g = \frac{2\pi}{h}$ and an equivalent refractive index is defined as $n_e = \frac{\lambda_0}{\lambda_g}$. Since only one conductor is involved, all angles of component plane waves are allowed for all values of k , i.e. all values of h and B are allowed, provided that

$$h^2 + B^2 = k^2 . \quad (5)$$

The situation changes, however, when the second conducting surface is in place, thus confining the energy into a certain region. The electric field between the two mirrors is the same as that for one mirror as long as their separation, d , satisfies the condition

$$\sin Bd = 0 . \quad (6)$$

For other values of d , the incident and reflected plane waves cannot satisfy the appropriate boundary conditions, and therefore equation (6) is a simple relationship between the allowed angles of propagation and waveguide thickness. This equation is sometimes called the characteristic equation for this structure. For a given thickness, d , of the guide, equation (6) determines a set of discrete values for B_n and also, by equation (5), a similar set for h_n . The roots B_0, B_1, B_2, \dots , combined with the field vector expressions, define the TE_0, TE_1, TE_2, \dots modes.

Another kind of mode is formed when the magnetic vector of the uniform plane waves is perpendicular to the plane of

incidence. In this case, the electric vector has a component parallel to the assumed direction of propagation as well as components transverse to the waveguide axis. Such modes are correspondingly described as transverse magnetic (TM) modes. TM modes between perfectly conducting surfaces have propagation constants satisfying the same conditions as TE modes.

The preceding analysis was taken after Kapany and Burke (Ref 1:8-11). A more classical approach to waveguide mode propagation involving the solutions of Maxwell's Equations can be found in Ref 1:14-34 and Ref 2:305-313.

Thus far, only a planar slab waveguide with perfectly conducting surfaces has been discussed, using a plane-wave approach. For fiber optics considerations, the interest lies in dielectric waveguides, which necessitate a description of additional modes. In a dielectric slab waveguide, modes which propagate can be considered as the superposition of two plane waves which remain inside the guide because of total internal reflection (this phenomena is described more thoroughly in the geometrical approach, pg.10). However, there is another set of modes in such a waveguide whose corresponding angles of incidence are equal to or less than the critical angle. These modes, said to be "cut off", give rise to evanescent surface waves. Evanescent waves occur when a field is forced to vary with a spatial period which is less than its free space propagation period. Such a situation is present when a wave attempts to enter into a medium whose dielectric constant (and thus its index of refraction) is less than that from which it came, i.e. total internal reflection (Ref 2:9). It will be seen later

that evanescent waves are useful in coupling energy from one waveguide to another. Other modes which do not propagate along the waveguide can be excited by any source of radiation or by discontinuities in the guide. They are also considered to be cut off because they decay as $e^{-\alpha z}$ away from such sources or or discontinuities (Ref 1:12, 13). Still another set of modes describe the resonant responses of the waveguide walls, such that the power in the guide decays exponentially in the z direction.

Before leaving the mode theory of dielectric waveguides, a comment on multimode and single mode waveguides is in order. As their names imply, a multimode waveguide is one which can support many modes at the same time, while a single mode waveguide can support only one mode. In terms of fiber optics, both single and multimode fibers exist, but this thesis will only be concerned with the multimode type.

It will be useful at this point to develop a simple model of a cylindrical optical fiber. This can be done using geometrical optics if the dimensions of the waveguide (fiber) are shown to be much greater than the wavelength of the light propagating in the waveguide (Ref 2:84). Since the multimode fibers used in this experiment have core diameters (.350mm) many times larger than the transmitted wavelength (630nm), an analysis using the geometrical ray approach appears to be valid.

A schematic drawing of a clad optical fiber is shown in Fig. 2. It consists of a core region of refractive index n_1 , surrounded by a cladding of lower refractive index n_2 . The medium surrounding the fiber is air, with refractive index

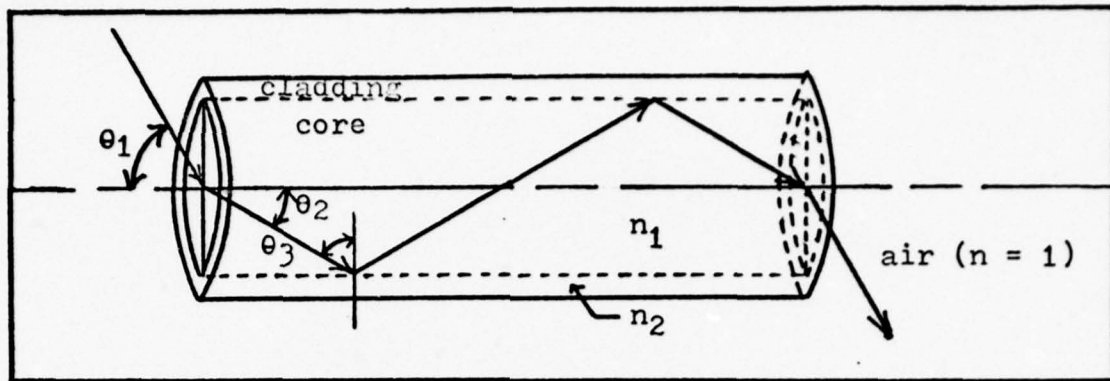


Fig. 2. Schematic of clad optical fiber

equal to 1. For a typical fiber made of two kinds of glass or plastic, $1 < n_2 < n_1$. Any ray of light crossing the boundary between the air and the fiber core with an angle of incidence θ_1 will be partially reflected and partially transmitted. The reflected ray will come off the boundary at an angle to the normal equal to θ_1 . This reflection is one source of fiber input loss which will be discussed later. Of interest at present is the transmitted ray, which makes an angle θ_2 with the normal. Using Snell's law,

$$\sin\theta_1 = n_1\sin\theta_2 \quad (7)$$

remembering that the index of air is equal to 1. Since $n_1 > 1$, θ_2 will always be less than θ_1 (Ref 3:38). Following the ray to where it meets the core-cladding interface, it is again partially reflected and partially transmitted. For the transmitted ray, Snell's law yields (see Fig. 3):

$$n_1\sin\theta_3 = n_2\sin\theta_4 \quad (8)$$

It can be seen that if the incident angle, θ_3 , has a critical

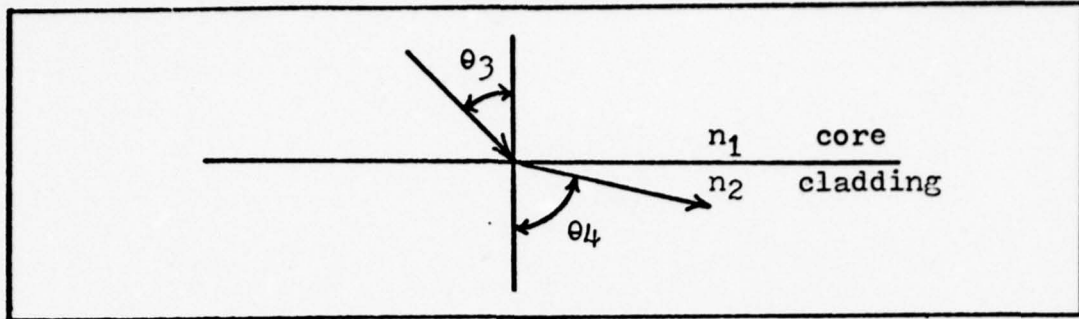


Fig. 3. Ray tracing at the core-cladding interface

value of θ_c which makes θ_4 equal to 90° , the transmitted ray becomes a surface wave along the core-cladding boundary. Total internal reflection occurs for $\theta_3 > \theta_c$, for which case the light remains inside the core. The expression for the critical angle is found from equation (8):

$$n_1 \sin \theta_3 = n_2 \sin \theta_4 \quad (8)$$

Let $\theta_4 = 90^\circ$, then $\theta_3 = \theta_c$, and

$$n_1 \sin \theta_c = n_2 \quad (9)$$

so that

$$\theta_c = \sin^{-1} \left(\frac{n_2}{n_1} \right) . \quad (10)$$

A meridional ray (i.e., one which intersects the axis of the cylindrical fiber) will be "trapped" inside the core and travel along via multiple total internal reflections as long as the angle it makes with the axis is less than $90^\circ - \theta_c$. From Fig. 2, the maximum value allowed for θ_2 is seen to be

$$\theta_{2 \text{ max}} = 90^\circ - \theta_c, \quad (11)$$

in order for the ray to travel inside the fiber core without

appreciable loss. It would be helpful to determine the maximum input angle of incidence, θ_1 , in terms of the refractive indices of the core and cladding. This is done by manipulating equation (11) such that

$$\sin(\theta_{2 \text{ max}}) = \sin(90^\circ - \theta_c) = \cos\theta_c . \quad (12)$$

From the basic trig identity

$$\sin^2\theta_c + \cos^2\theta_c = 1 , \quad (13)$$

it is seen that

$$\sin(\theta_{2 \text{ max}}) = \left[1 - \sin^2\theta_c \right]^{\frac{1}{2}} . \quad (14)$$

Now, from equation (10),

$$\sin\theta_c = \left(\frac{n_2}{n_1} \right) \quad (15)$$

and

$$\sin^2\theta_c = \left(\frac{n_2}{n_1} \right)^2 . \quad (16)$$

Substituting into equation (14),

$$\sin(\theta_{2 \text{ max}}) = \left[1 - \left(\frac{n_2}{n_1} \right)^2 \right]^{\frac{1}{2}} . \quad (17)$$

Rewriting equation (17),

$$\sin(\theta_{2 \text{ max}}) = \left[\frac{n_1^2 - n_2^2}{n_1^2} \right]^{\frac{1}{2}} = \frac{1}{n_1} \left[n_1^2 - n_2^2 \right]^{\frac{1}{2}} , \quad (18)$$

so that

$$n_1 \sin(\theta_{2 \text{ max}}) = \left[n_1^2 - n_2^2 \right]^{\frac{1}{2}} . \quad (19)$$

But from equation (7),

$$\sin\theta_1 = n_1 \sin\theta_2 , \quad (7)$$

so that the maximum angle of incidence which still assumes total internal reflection propagation is

$$\theta_1 \text{ max} = \sin^{-1} \left[n_1^2 - n_2^2 \right]^{\frac{1}{2}} . \quad (20)$$

This brings about the definition of a limiting numerical aperture (NA) of a fiber. The NA of any ray is (Ref 4:68)

$$NA = n_1 \sin\theta_2 = (1) \sin\theta_1 , \quad (21)$$

and the limiting NA of a fiber can be defined as

$$NA_f = (1) \sin(\theta_1 \text{ max}) = \left[n_1^2 - n_2^2 \right]^{\frac{1}{2}} . \quad (22)$$

Similar derivations of the NA of a fiber are found in Ref 4:145-148 and Ref 5:8.

Note that since Snell's law applies to both ends of the fiber, any ray advancing along the core with $\theta_1 < \theta_1 \text{ max}$ will exit the fiber at the same angle, θ_1 , at which it entered (Ref 4:148).

The preceding discussion has dealt strictly with meridional rays in a straight fiber. There are other rays in such a cylindrical waveguide which do not intersect the axis of the fiber and are called skew rays. These rays travel in helical paths as they are conducted along the fiber and are subject to the same conditions as meridional rays when traveling: $\theta_1 < \theta_1 \text{ max}$ for total internal reflection (Ref 4:149). A formal treatment of skew rays is quite involved and will not be attempted here (see Ref 1:96-99, and Ref 2:289-305).

Coupler Design

The second portion of this theoretical section deals with the design criteria for various kinds of fiber optic couplers. After a brief discussion on the aspects of energy exchange between two parallel fibers, an application of this idea is made to single fiber directional and tee couplers. Next, the design of a scrambler, or mixing rod for star couplers is developed. Following that will be an analytical discussion of loss factors to be expected in coupler fabrication and operation.

When considering the coupling of energy from one dielectric waveguide to another in close proximity to it, a detailed analysis can become quite lengthy. The following discussion is therefore qualitatively oriented with references given for the more involved ideas. As mentioned earlier, when electromagnetic waves in a waveguide undergo total internal reflection at the core-cladding boundary (e.g. an optical fiber), there is (in addition to the reflected wave) an evanescent surface wave which penetrates the cladding and which decays exponentially in the direction transverse to the waveguide axis. It is this evanescent wave which gives rise to a method of coupling energy between waveguides (Ref 2:407). When two identical waveguides are laid parallel to each other and the first one is excited by a radiation source, the evanescent wave thus formed can reach into the second waveguide and in turn excite it. This phenomenon is analogous to the method of mode launching in dielectric thin films using frustrated total reflection (Ref 2:408). Briefly, this method uses a prism of refractive index n_1 placed near a thin film of the same index which is

surrounded by a lower index material (n_2) as shown in Fig. 4. An incident beam on the prism will be nearly totally reflected at the first $n_1 - n_2$ interface except for the small evanescent field which passes through the n_2 layer and sets up propagating modes in the higher index thin film (Ref 1:36-38).

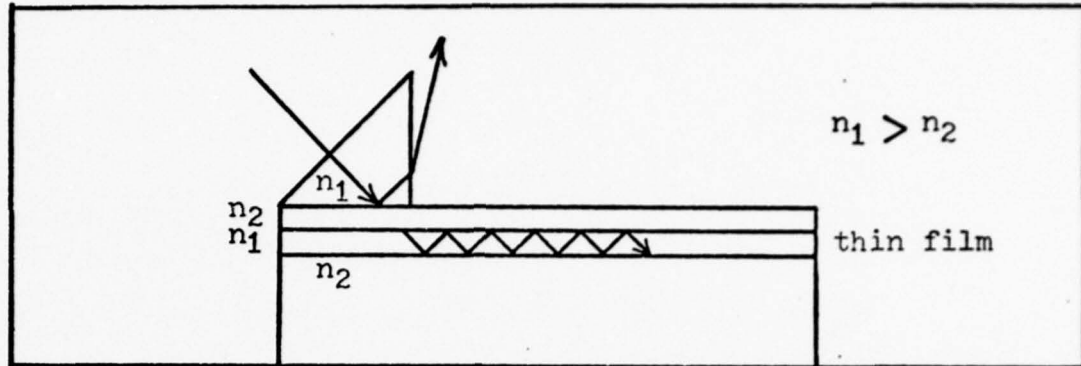


Fig. 4. Schematic of frustrated total reflection prism-thin film coupler

Since evanescent coupling in parallel waveguides tends to be unidirectional, i.e. the power transferred travels the same direction in each guide (Ref 2:409), an application is apparent for the design of directional and tee couplers. In addition, the amount of power transferred depends upon the interaction length (Ref 1:234) and the coupling ratio can therefore be varied to suit the situation at hand. A single strand, multimode tee coupler employing the above coupling technique has been fabricated by M. K. Barnoski and H. R. Friedrich of Hughes Research Laboratories (Ref 6) and will be analyzed in the first portion of the experimental section.

Consider now a different coupling technique, one which requires the design of a light scrambler or mixing rod which is larger in diameter than each individual fiber, and into

which two or more fibers are fed. It will be shown later that such a mixing rod can be used in the fabrication of a directional, tee or star coupler. The basic idea of this technique involves the transfer of the output from one fiber to the mixing rod and subsequent transfer from there to the other fibers in the system.

The main criteria in the design of the mixing rod is the requirement that the cone of light coming from the end of the input fiber is spread across the entire width of the rod. Therefore, some optimum length-versus-width ratio must be described, depending upon the numerical aperture of the individual fibers and the mixing rod material. Fig. 5 shows the limiting case where the input fiber is located at one edge of the

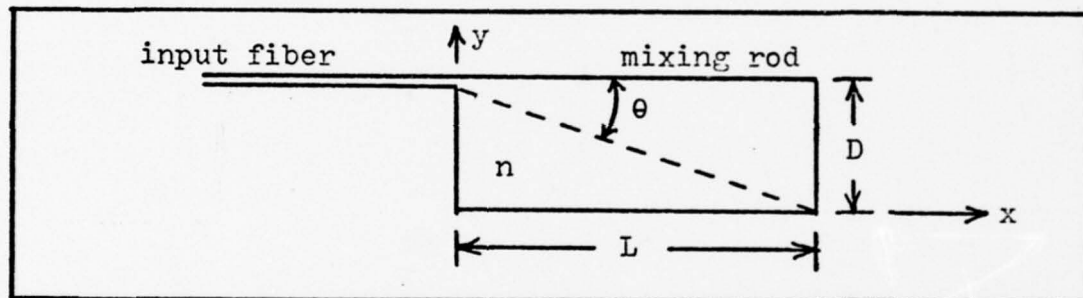


Fig. 5. Schematic of mixing rod design consideration

mixing rod. Proper design requires that one half of the fiber's output cone spreads across the diameter $y=D$ in the length $x=L$. One half the output cone is just the limiting numerical aperture of the fiber, taken from equation (22):

$$NA_f = n \sin \theta . \quad (23)$$

Now, starting from the trig identity,

$$\cos \theta = (1 - \sin^2 \theta)^{\frac{1}{2}} , \quad (24)$$

and multiplying by $\frac{n}{n}$,

$$\cos\theta = \frac{1}{n}(n^2 - n^2\sin^2\theta)^{\frac{1}{2}} , \quad (25)$$

the substitution of equation (23) gives

$$\cos\theta = \frac{1}{n}[n^2 - (NA_f)^2]^{\frac{1}{2}} . \quad (26)$$

Next, consider the trig identity,

$$\tan\theta = \frac{\sin\theta}{\cos\theta} . \quad (27)$$

Substituting equation (26),

$$\tan\theta = \frac{n\sin\theta}{[n^2 - (NA_f)^2]^{\frac{1}{2}}} \quad (28)$$

and using equation (23) again,

$$\tan\theta = \frac{NA_f}{[n^2 - (NA_f)^2]^{\frac{1}{2}}} . \quad (29)$$

Finally since

$$\tan\theta = D/L , \quad (30)$$

then the required design equation is

$$\frac{D}{L} = \frac{NA_f}{[n^2 - (NA_f)^2]^{\frac{1}{2}}} \quad (31)$$

Equation (31) is suitable for a coupler with an input fiber on one end of the mixing rod and output fibers on the other end. Application of this design would be useful for directional or tee couplers where the energy would spread from one fiber to two as it passed through the rod as in Fig. 6. A star coupler, however, requires a slight modification of the design equation. A simple star coupler has all of its component fibers

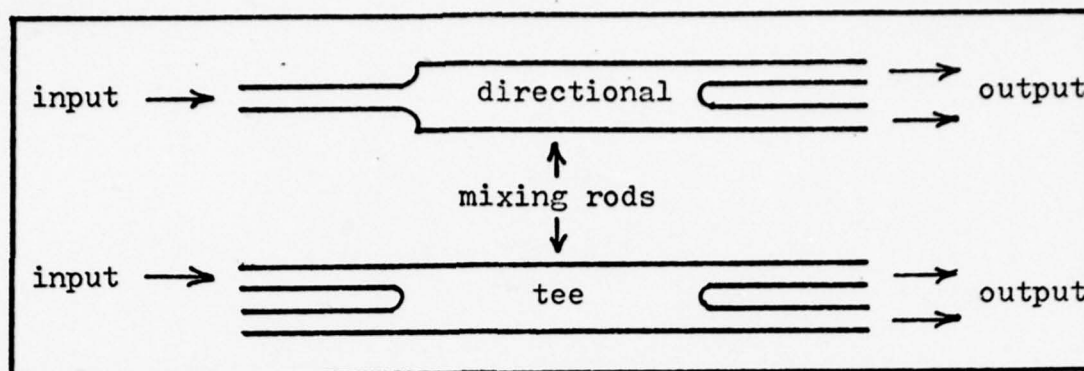


Fig. 6. Directional and tee couplers using mixing rod

on one end of the mixing rod while the other is coated with some sort of mirrored surface (Fig. 7). Since the light from any fiber will undergo a reflection from the mirror surface, the cone of light will cover the entire diameter (in the limiting case) in only one-half the length required for the previous design. Therefore, equation (31) is modified for a star coupler:

$$\frac{D}{L} = 2 \left[\frac{NA_f}{n^2 - (NA_f)^2} \right]^{\frac{1}{2}} \quad (32)$$

The preceding analysis was taken after the discussion in Ref 4:67-71.

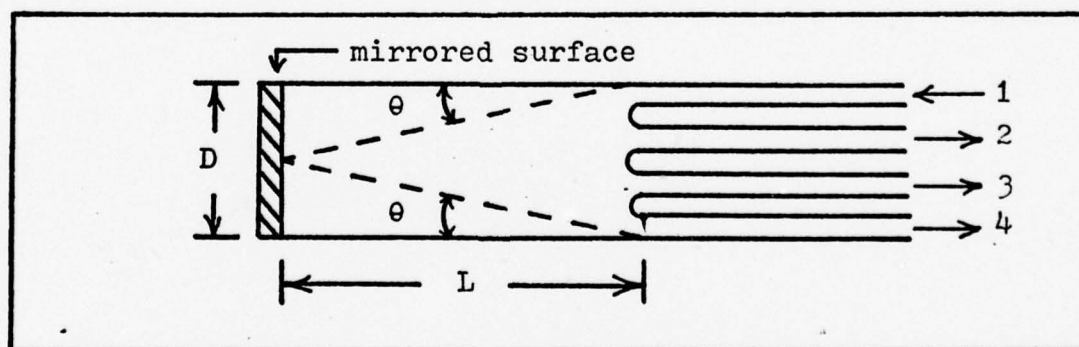


Fig. 7. Star coupler design (4-port)

A few words must now be said concerning the various losses to be expected when measuring the performance of an experimental

coupler. For single strand, multimode fiber couplers, these losses include attenuation in the various dielectric materials involved, packing fraction losses (at the fiber-mixing rod boundary in star couplers), and reflective losses at each interface, whether it be an air-to-fiber boundary, a fiber-to-fiber boundary, or a fiber-to-mixing rod boundary. Reflective losses are the most prominent in optical coupler work and will be discussed in some detail.

To determine a relation which will indicate how much power is lost by reflection when an electromagnetic wave passes across the boundary between two dielectric media of refractive indices n_1 and n_2 , consider Fig. 8. The following list explains the symbols used (Ref 3:38-39):

- \vec{S} : Poynting vector of incident wave
- $A_{||}$: Complex amplitude of incident electric vector parallel to plane of incidence
- A_{\perp} : Complex amplitude of incident electric vector perpendicular to plane of incidence
- $T_{||}$: Complex amplitude of transmitted wave parallel to plane of incidence
- T_{\perp} : Complex amplitude of transmitted wave perpendicular to plane of incidence
- $R_{||}$: Complex amplitude of reflected wave parallel to plane of incidence
- R_{\perp} : Complex amplitude of reflected wave perpendicular to plane of incidence

The well-known Fresnel formulas for the transmitted and reflected components are the following (Ref 3:40):

$$T_{||} = \frac{2n_1 \cos \theta_i}{n_2 \cos \theta_i + n_1 \cos \theta_t} A_{||} \quad (33)$$

$$T_{\perp} = \frac{2n_1 \cos \theta_i}{n_1 \cos \theta_i + n_2 \cos \theta_t} A_{\perp} , \quad (34)$$

$$R_{\parallel} = \frac{n_2 \cos \theta_i - n_1 \cos \theta_t}{n_2 \cos \theta_i + n_1 \cos \theta_t} A_{\parallel} , \quad (35)$$

$$R_{\perp} = \frac{n_1 \cos \theta_i - n_2 \cos \theta_t}{n_1 \cos \theta_i + n_2 \cos \theta_t} A_{\perp} . \quad (36)$$

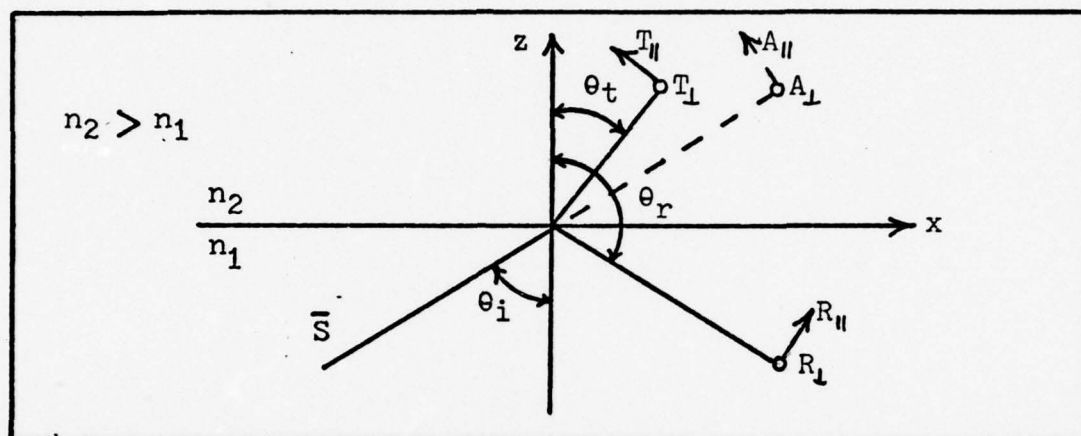


Fig. 8. Diagram of EM wave incident on boundary between two dielectric media (Ref 5:38)

For the purposes of the couplers evaluated in this experiment, the above equation will be simplified by assuming normal incidence. Therefore $\theta_i = 0$ and $\theta_t = 0$, reducing the Fresnel formulas to (Ref 3:41):

$$\left. \begin{aligned} T_{\parallel} &= \frac{2}{n+1} A_{\parallel} \\ T_{\perp} &= \frac{2}{n+1} A_{\perp} \end{aligned} \right\} \quad (37)$$

$$\left. \begin{aligned} R_{\parallel} &= \frac{n-1}{n+1} A_{\parallel} \\ R_{\perp} &= -\frac{n-1}{n+1} A_{\perp} \end{aligned} \right\} \quad (38)$$

where $n = \frac{n_2}{n_1}$. At this point, two important parameters can be defined. They are the transmissivity (t) and reflectivity (r) given in general by:

$$t = \frac{n_2 \cos \theta_t |T|^2}{n_1 \cos \theta_i |A|^2} \quad (39)$$

and

$$r = \frac{|R|^2}{|A|^2} \quad (40)$$

where $|A|$, $|T|$, and $|R|$ are the magnitudes of the incident, transmitted, and reflected vectors, respectively. Again simplifying for normal incidence, these parameters reduce to (Ref 3:42):

$$t = \frac{4n}{(n + 1)^2} \quad (41)$$

and

$$r = \left(\frac{n - 1}{n + 1} \right)^2 \quad (42)$$

where again, $n = \frac{n_2}{n_1}$. Equation (42) is the factor commonly used in fiber optics to determine reflective losses at each interface (Ref 7).

Another source of losses, attenuation in the dielectric materials used in fabrication, consists of absorption loss (intrinsic, impurity, and atomic defect) and scattering loss due to thermal fluctuation of atoms, Raman scattering, Brillouin scattering, and waveguide structure (Ref 1:26-31). These effects are usually not noticable unless the length of the fiber system is large. In dealing with optical couplers, then, the only concern for material losses will be in obvious defects

observed, for example, in the mixing rod of the star couplers.

Packing fraction losses at the fiber-mixing rod boundary are another concern. Since the face of the mixing rod can be considered continuous as compared to the collective face of the group of fibers adjacent to it, a certain amount of light will exit the rod and not be collected by one of the fibers. This sort of loss is called packing fraction loss and can be evaluated using the relation

$$L_{p.f.} = \frac{A_f}{A_r} \quad (43)$$

where $L_{p.f.}$ is loss due to packing fraction, A_f is the combined cross-sectional area of the individual fibers, and A_r is the cross-sectional area of the mixing rod.

EXPERIMENTAL

Equipment and Set-up

The experimental section of this thesis consists of the qualitative description and quantitative measurement of various kinds of fiber optic couplers. The first portion deals with the equipment and set-up involved in measuring fiber diameters and other coupler dimensions. The second portion will discuss the set-up used in measuring coupler performance, and will describe the purpose and specifications (as needed) of each element in the optical train. The next portion will deal with the actual couplers measured and the data obtained. The couplers considered include a single-fiber fused tee from Hughes Research Laboratories, and eight-port fiber bundle star from Spectronics, and several single-fiber tee and star designs fabricated specifically for this experiment.

All measurements of the physical dimensions of any fiber optic component used in this experiment were made using the following equipment:

- a) "Stereozoom" Microscope: Bausch and Lomb
- b) Upper light source: American Optical Co.
- c) Lower light source: Bausch and Lomb, 31-35-30
- d) Reticle: Bausch and Lomb micrometer disc, 31-16-08
(1 division = 0.001 inch)
- e) Polaroid Camera attachment: Bausch and Lomb
- f) Film: Polaroid type 107 (B/W)

The microscope and other equipment was set up as shown in Fig. 9.

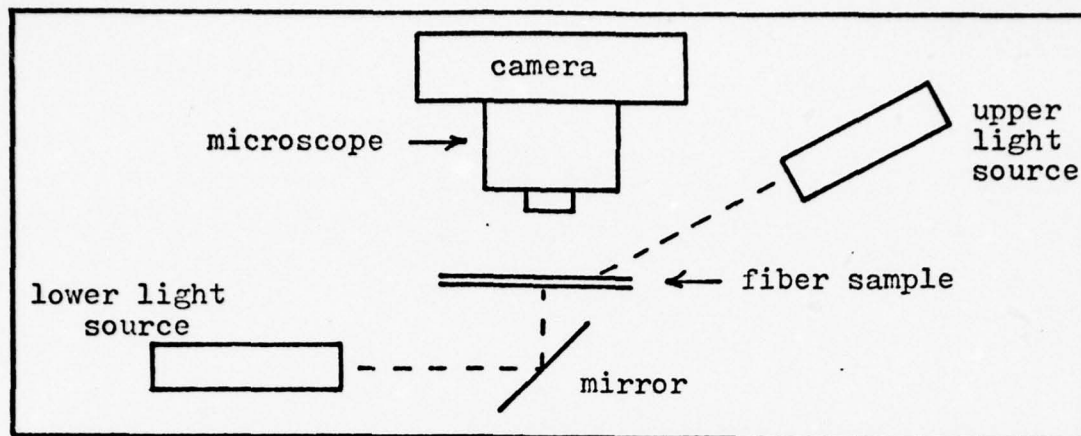


Fig. 9. Set-up for fiber dimension measurement

For actual coupling efficiency measurements, the following equipment was used:

- a) HeNe laser: Spectra Physics
- b) Chopper: Bulova 150Hz
- c) Microscope objective lens: 16mm, NA 0.25
- d) Pinhole: 10 microns in diameter, Jodon Engineering
- e) Lenses #1: $f = 17\text{cm}$
 #2: $f = 17\text{cm}$
 #3: $f = 22\text{cm}$
- f) Detector: HP p-i-n photodiode, 5082-4205
- g) Oscilloscope: Tektronix type 555

For all experimental measurements, the following set-up (Fig. 10) was used, the detector being flexible in placement depending upon which type of coupler was being evaluated. Any changes made in this general set-up will be noted for the particular coupler under consideration.

Each item listed above plays a role in the measurement process, and the reasons for the inclusion of each will now be discussed. To begin with, the laser provides a strong source

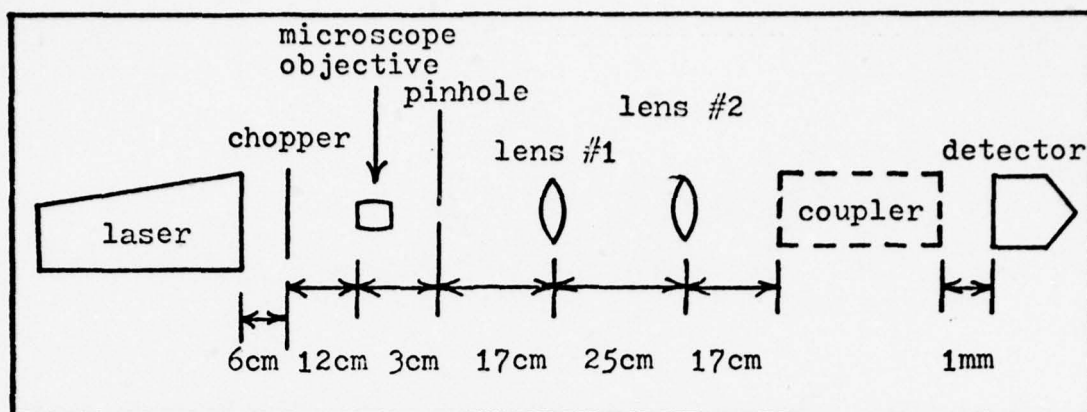


Fig. 10. Experimental set-up for coupler efficiency measurement

of radiation in the visual wavelength region (6328\AA), and can therefore be easily observed. More typically, fiber optic systems employ light emitting diodes or laser diodes (two specific wavelengths are 0.86 microns and 1.06 microns) as their sources. However, the laser used here is a convenient one, requiring no physical contact with the fibers themselves.

Once out of the laser cavity, the light beam encounters the 150Hz chopper whose sole purpose is to provide square wave triggering for the oscilloscope. The laser and chopper act like a signal source in an actual fiber optic system, and the relative amplitude of the square wave is an excellent indication of how much energy is being transferred through the coupler.

Immediately following the chopper is a short focal length microscope objective which focuses the beam down to the 10 micron pinhole. This aperture provides a point source from which spherical waves are emitted. The distance between the microscope objective and the pinhole was adjusted such that only

the central disc portion of the Airy pattern was transmitted. Since the pinhole was placed at the focal length of lens #1, the emerging beam from that lens was essentially collimated, consisting of plane waves. Placement of lens #2 could then be varied, thus focusing the beam back down at any point along the optical bench, its placement depending upon the size and position of the coupler to be tested.

The coupler itself would be oriented such that the end of its input fiber (i.e. the fiber to be initially excited) was at the focal point of lens #2. Ideally, the focal length of lens #2 should be chosen such that the cone of converging rays match the numerical aperture (NA) of the input fiber. For the purpose of this experiment, however, the lens was chosen so as to insure that the effective NA of the lens was less than the NA of the input fiber, thereby allowing a maximum amount of energy into the fiber.

Finally, a detector is placed at the output of the coupler, approximately 1mm from the end of the fiber in question. This particular p-i-n photodiode was chosen for its small surface area (0.02mm^2), hemispherical lens, and good response in the visible wavelength region. This detector is connected directly to the oscilloscope, which provides a visual, quantitative reference for coupler efficiency measurement.

Hughes Tee Coupler Evaluation

The first coupler to be considered is one of the tee variety developed for the Air Force (#F33615-75C-1024) by M. K. Barnoski and H. R. Friedrich of Hughes Research Laboratories,

Malibu, California. In addition to providing a test object for the optical set-up described above, measurements of the device's coupling efficiency will be compared to published results (Ref 6:2630) and supplied as reference information to the Avionics Laboratory. This particular tee coupler consists of two single-strand, multimode fiber waveguides which have been thermally fused side by side along a given interaction length by a focused CO₂ laser. The fibers were supplied by Corning and have a core diameter of 85 microns, with a 0.14 numerical aperture (Fig. 11). The objective of this eval-

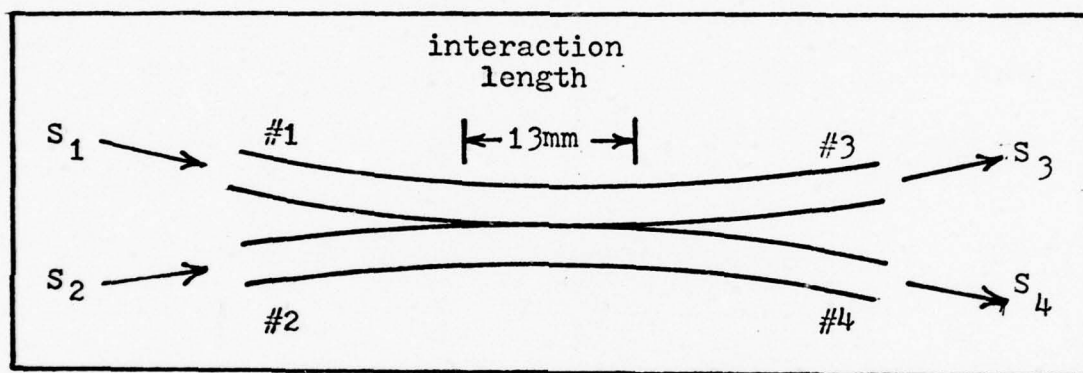


Fig. 11. Schematic of Hughes single fiber fused tee coupler

uation is to determine the coupling efficiency from one of the waveguides to the other (an example of parallel waveguide interaction). To do this, one of the fibers is excited and the output from the other three is measured. Using the obtained data, two evaluation parameters can be determined. The first, defined as the tap ratio, is given as (Ref 6:2630):

$$C_{14} = \frac{S_4}{S_1} \quad , \quad (44)$$

where S_4 is the signal measured from fiber #4 and S_1 is the

input fiber (#1) signal. The second parameter is called the excess insertion loss, defined as (Ref 6:2630):

$$L_1 = 10 \log \left(\frac{S_4 + S_3}{S_1} \right) , \quad (45)$$

where S_4 and S_1 are defined above, and S_3 is the signal measured in fiber #3. The procedure used was the following:

- a) The coupler was placed in the test set-up such that the end of fiber #1 was located at the focal point of lens #2.
- b) The laser was turned on and the output from each fiber was observed.
- c) The detector was placed at the end of each fiber (#2, #3, and #4) in turn, and the output reading on the scope was recorded.
- d) The above procedure was repeated three times, each time using a different fiber as the input.

Observation of the coupler under excitation revealed fairly strong outputs from the two fibers opposite the input fiber, and a weak signal coming from the fiber located on the same side as the input fiber. Although evanescent coupling between parallel waveguides is essentially unidirectional, the weak output from the third fiber is most likely due to a reflection from its opposite end. The data taken is summarized in Table I.

Typical published results (Ref 6:2630) for this type of coupler are:

$$C_{14} = 6.6\% (-11.8 \text{ dB})$$

and

$$L_1 = -1.1 \text{ dB} .$$

Table I

Data taken from Hughes Tee Coupler HTC-32

Input Fiber	Output Fiber	Output, mV (Peak-to-Peak)	Tap Ratio	Excess Insertion Loss
1	2	not measurable	$C_{14} = 9\%$	$L_1 = -4.6 \text{ dB}$
	3	36.0	(-10.7 dB)	
	4	12.0		
2	1	0.1	$C_{23} = 3\%$	$L_2 = -4.9 \text{ dB}$
	4	42.0	(-14.6 dB)	
	3	4.8		
3	4	not measurable	$C_{32} = 4\%$	$L_3 = -8.0 \text{ dB}$
	1	17.0	(-14.5 dB)	
	2	5.0		
4	3	0.3	$C_{41} = 16\%$	$L_4 = -3.3 \text{ dB}$
	2	44.0	(-8.0 dB)	
	1	22.0		

Input fiber signal: 140mV (obtained by placing detector at focal point of lens #2).

While the results obtained in this experiment are near the same general value, perhaps something should be said about the variance seen when using different input fibers. It is likely that the factor most effecting this discrepancy was the

critical alignment of the source beam and input fiber. The inability to position the two exactly the same way for each trial resulted in varying coupling efficiencies. The detector's alignment was also important, and because of the individual fibers' fragility, the detector-to-output fiber distance could only be approximated ($\sim 1\text{mm}$), thus adding to the non-uniformity of results.

In an attempt to determine the source of the weak signal emitted from the coupled fiber on the input side of the coupler (interface b in Fig. 12), consider the internal reflections present. In the coupled fiber, the two signals S_t and S_o are known from experimental measurement. The value of S_r

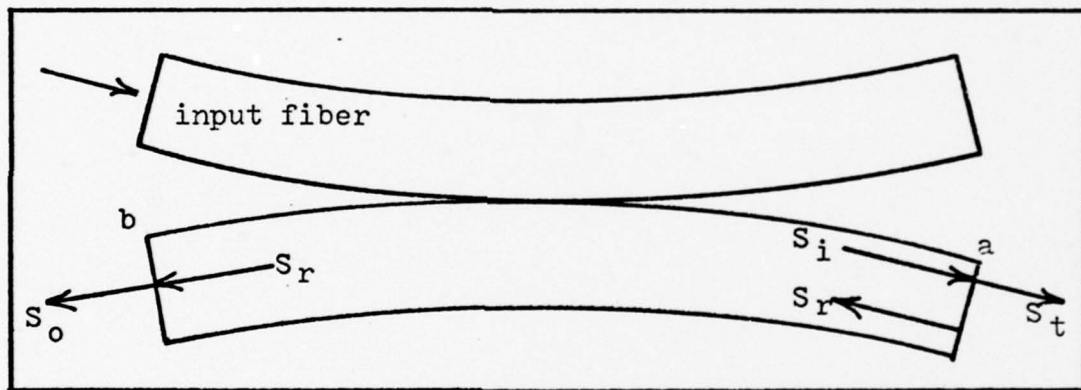


Fig. 12. Internal reflections in coupled fiber

must be found upon exit and compared to S_o . Using equation (42), the reflective loss at any interface can be written as

$$r = \left(\frac{n_1 - n_2}{n_1 + n_2} \right)^2 = 0.04 \quad (46)$$

where n_1 is the refractive index of the core ($= 1.5$ in this case), and n_2 is the refractive index of the outside medium ($= 1.0$ for air). At interface a, it is seen that

$$(S_i)(r) = S_r \quad (47)$$

and

$$S_r + S_t = S_i \quad (48)$$

Substituting for S_i in equation (48) gives

$$S_r + S_t = \frac{S_r}{r} \quad (49)$$

Solving for S_r ,

$$S_r = \frac{S_t}{\frac{1}{r} - 1} \quad (50)$$

To compare S_r outside the fiber to the measured S_o , the reflective loss at interface b must also be considered. Therefore, S_r (outside) would be

$$S_r(\text{outside}) = S_r(1-r) \quad (51)$$

As an example, consider the data taken when fiber #2 was used as the input fiber. In this case,

$$S_t = S_3 = 4.8\text{mV} \quad (52)$$

and

$$S_o = S_1 = 0.10\text{mV} \quad (53)$$

From equation (50),

$$S_r = \frac{4.8\text{mV}}{\frac{1}{0.04} - 1} = 0.2\text{mV} \quad (54)$$

and from equation (51),

$$S_r(\text{outside}) = (0.2\text{mV})(1 - 0.04) = 0.19\text{mV} \quad (55)$$

Similar calculations done for the case where fiber #4 was the input fiber result in the following:

$$S_0 = S_3 = 0.3\text{mV} \quad (56)$$

and

$$S_r(\text{outside}) = 0.87\text{mV} \quad (57)$$

These figures indicate that the faint outputs observed are most likely due to the internal reflections in the coupled fiber. The measured output (S_0) was probably not as high as the predicted one ($S_r(\text{outside})$) due to other losses such as coupling back into the input fiber (Ref 1:57).

Spectronics Star Coupler Evaluation

The second coupler evaluated is a radial one, or star coupler fabricated by Spectronics, Inc., of Richardson, Texas (Ref 4:111-126). It consists of eight input/output ports and employs fiber bundles for its radial arms. Although this study was intended to cover single fiber devices exclusively, it was thought the testing of this presently available coupler would provide a good experimental basis in dealing with multi-port star designs. Details of the coupler itself are shown in Fig. 13.

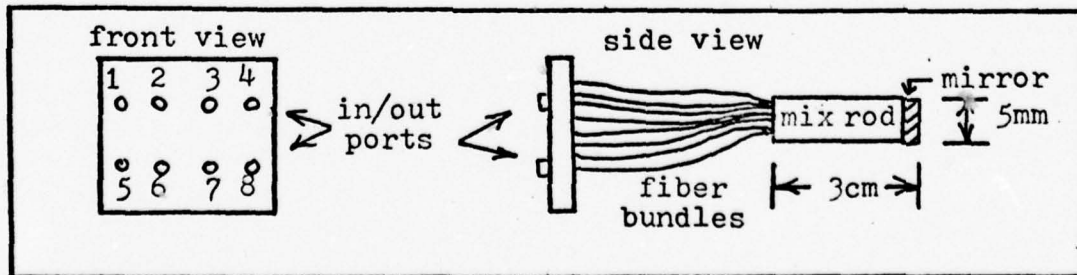


Fig. 13. Eight-port star coupler

The set-up for evaluating this device's coupling efficiency is essentially the same as that in the previous section, except for the detector position (since all in/out ports are facing the same direction as in Fig. 14).

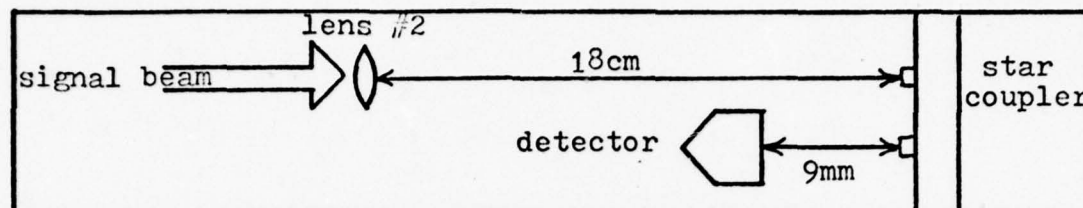


Fig. 14. Star coupler placement in test apparatus

In a tee coupler, where the ratio between the two output ports can be varied, the important parameter is the tap ratio. A star coupler, on the other hand, is evaluated for its uniformity of output, regardless of which port is used as the input. Therefore, an important evaluation for a star coupler will be in observing nearly equal outputs from all ports, and determining whether or not that observed value changes when varying the input ports. The above evaluation is made with the help of the transmission factor which is defined as (Ref 4:51)

$$T_* = \frac{(\text{signal at output port})}{(\text{signal at input port})} \quad (58)$$

This factor can be compared to the tap ratio in tee couplers. A second measurement parameter dealing with the optical losses of the coupler can be defined as the insertion loss (similar to the excess insertion loss of the tee coupler):

$$L_* = 10 \log \frac{(\text{total signal from all output ports})}{(\text{signal at input port})} \quad (59)$$

The procedure used in this portion of the experiment is as follows:

- a) The coupler was placed in the optical set-up such that port #1 was in the beam path.
- b) The distance between the coupler and lens #2 was adjusted such that the spot size of the beam just matched the diameter of the fiber bundle at port #1 (~1.5mm). This was done to insure uniform illumination of the entire bundle.
- c) The detector was placed in front of each of the other ports, in turn, and the resulting signal recorded from the oscilloscope.
- d) The above procedure was repeated seven times, each time using a different port as the input.

Results of the above coupler test are summarized in Table II. Note that this table also supplies some published results obtained from the same kind of star coupler (Ref 4:119,125). The similarity between data is merely an indication that the experimental set-up and procedure used are viable in evaluating couplers of this sort.

Experimentally Fabricated Couplers

The foregoing analysis and experience gained allow the fabrication and evaluation of several types of fiber optic couplers. The general method of write-up for each coupler will be (1) a description of materials used and fabrication techniques involved, (2) a summary of data taken, and (3) a discussion of results. The equipment and set-up used previously

Table II

Data taken from Spectronics Star Coupler

Input Fiber	Output Fiber	Output, mV (Peak-to-Peak)	T* (Measured)	T* (Published)	L* (Measured)
1	2	0.55	0.03	0.02	-7.7 dB
	3	0.40	0.02	0.05	
	4	0.45	0.02	0.04	
	5	0.55	0.03	0.04	
	6	0.40	0.02	0.05	
	7	0.50	0.03	0.02	
	8	0.30	0.02	0.03	
2	1	1.40	0.07	0.02	-2.84 dB
	3	3.00	0.15	0.02	
	4	0.35	0.02	0.02	
	5	3.00	0.15	0.04	
	6	1.50	0.08	0.01	
	7	0.02	0.01	0.07	
	8	0.80	0.04	0.03	
3	1	0.75	0.04		-4.32 dB
	2	0.35	0.02		
	4	2.00	0.10		
	5	0.20	0.01		
	6	1.20	0.06		
	7	1.25	0.07		
	8	1.30	0.07		
4	1	0.14	0.01		-10.0 dB
	2	0.32	0.02		
	3	0.12	0.006		
	5	0.16	0.01		
	6	0.35	0.02		
	7	0.08	0.004		
	8	0.60	0.03		
5	1	0.50	0.03		-7.96 dB
	2	0.50	0.03		
	3	0.40	0.02		
	4	0.50	0.03		
	6	0.30	0.02		
	7	0.30	0.02		
	8	0.20	0.01		
6	1	1.80	0.09		-2.84 dB
	2	2.00	0.10		
	3	1.60	0.08		
	4	1.60	0.08		
	5	1.00	0.05		
	7	0.90	0.05		
	8	0.70	0.07		

(continued on next page)

Table II
(continued)

Input Fiber	Output Fiber	Output, mV (Peak-to-Peak)	T* (Measured)	T* (Published)	L* (Measured)
7	1	2.00	0.10		
	2	0.50	0.03		
	3	2.70	0.14		
	4	1.10	0.06		-3.57 dB
	5	0.40	0.02		
	6	1.00	0.05		
	8	1.60	0.08		
8	1	0.15	0.01	0.03	
	2	0.30	0.02	0.02	
	3	0.30	0.02	0.03	
	4	0.35	0.02	0.02	-10.46 dB
	5	0.08	0.004	0.03	
	6	0.25	0.01	0.02	
	7	0.12	0.006	0.03	
Input fiber bundle signal: 20mV					

will again be employed in testing the devices made. The parameters used for evaluation will also be the same as described above (tap ratio, transmission factor, and insertion loss). Discussion of results will include possible reasons for optical losses, problems in various methods of fabrication, and comparison between designs.

a) Directional Couplers (DC-1,DC-2)

The first device made was a directional coupler (one input fiber and two output fibers) which employs a quartz mixing rod. This coupler was made as a single unit in that the input and output fibers were pulled directly from a solid quartz cylinder, which served as the mixing rod. The limiting dimensions on the coupler were obtained from equation (31), using $n = 1.5$ (quartz) and $NA_f = 0.96$. Since the fibers were unclad quartz, the NA_f was obtained experimentally in the

following way:

- a) A sample section of quartz fiber was placed such that a focused laser beam entered one end.
- b) A white card was placed perpendicular to the fiber's axis at $x = 12.7\text{mm}$ from the opposite end of the fiber, such that the output of the fiber could be seen as a bright circular spot on the card.
- c) The radius (r) of the circular spot (from the center out to the point where the intensity had diminished by approximately 90%) was measured to be 9.5mm as shown in Fig. 15.
- d) The numerical aperture of the fiber was calculated from equation (22):

$$NA_f = n \sin \theta = (1.0) \sin(\tan^{-1} \frac{r}{x}) = 0.60 \quad (60)$$

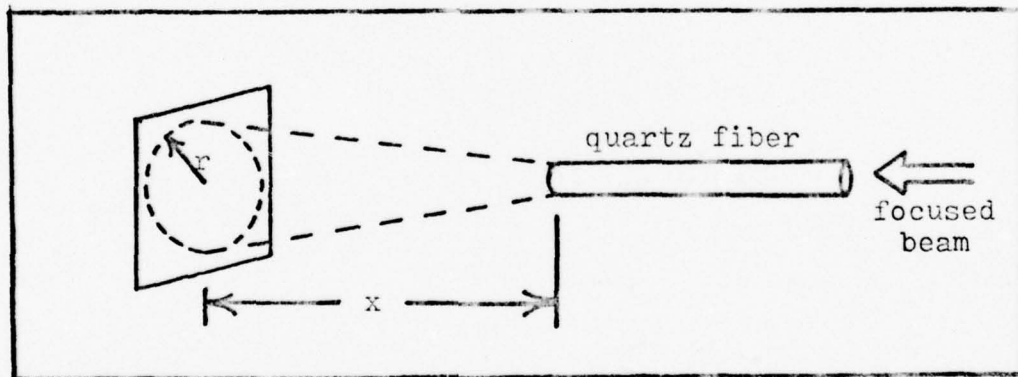


Fig. 15. Experimental measurement of NA_f

According to the design equation (31) for this kind of mixing rod, the ratio of length to width is

$$\frac{L}{D} = \frac{[(1.5)^2 - (.60)^2]^{\frac{1}{2}}}{.60} = 2.29 \quad (61)$$

The above ratio is the limiting case for proper mixing rod

operation. The actual dimensions used were governed by availability of materials and ease of fabrication. Therefore, the coupler was made beginning with a solid quartz rod 35mm long and 2mm in diameter. The three necessary fiber ports were drawn from this rod by typical glass working techniques using an oxygen fed torch. A schematic of the finished product is shown in Fig. 16. Dimensions of the individual fibers were measured microscopically using the procedure outlined on pages 24 and 25.

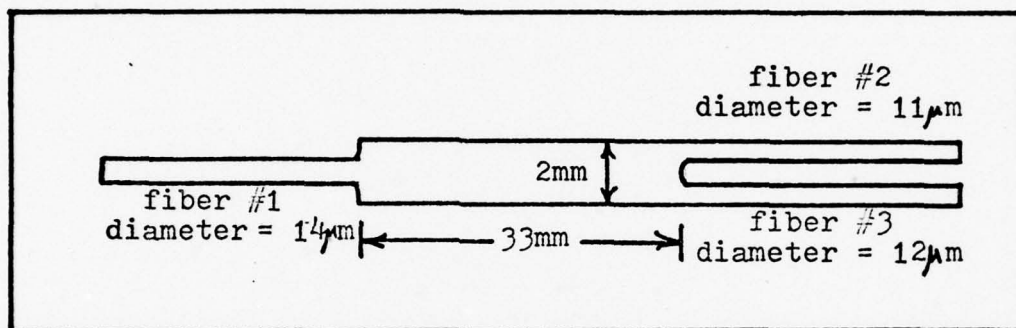


Fig. 16. Schematic of DC-1

Fig. 17 shows a photograph (taken through the microscope) of the output side of the directional coupler (fibers #2 and #3). Non-uniformity of the fiber's size and deformation of the mixing rod can be attributed to glass working difficulties in dealing with such a small device. Fig. 19 is a photograph of DC-1 being tested in the experimental set-up. The procedure for testing was as follows:

- a) The coupler was placed in the test set-up such that the end of fiber #1 was located at the focal point of lens #2.
- b) The laser was turned on and the output from the other two fibers was observed.

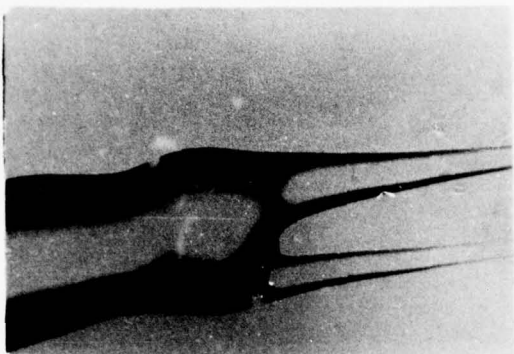


Fig. 17. Output side of DC-1

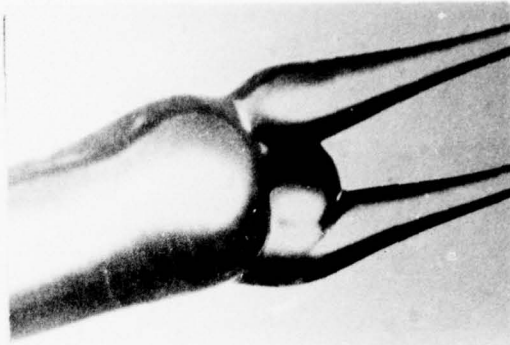


Fig. 18. Output side of DC-2

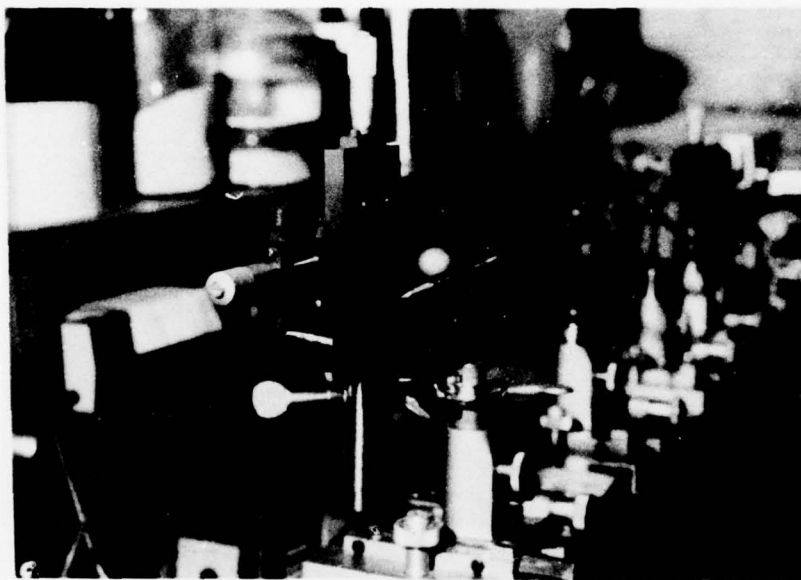


Fig. 19. DC-1 in experimental set-up

- c) The detector was placed at the end of fiber #2 and fiber #3, in turn, and the output reading on the scope was recorded.
- d) The coupler was turned around and the output from fiber #1 was recorded when using fiber #2 and fiber #3, in turn, as the input fiber.

The resulting data is summarized in Table III.

Table III
Data from Directional Coupler DC-1

Input Fiber	Output Fiber	Output, mV (Peak-to-Peak)	Tap Ratio	Excess Insertion Loss
1	2	0.6	$C_{12} = 0.3\%$ (-25.2 dB)	$L_1 = -18.3$ dB
	3	2.2	$C_{13} = 1.2\%$ (-19.4 dB)	
2	1	1.6	$C_{21} = 0.8\%$ (-20.7 dB)	
3	1	0.25	$C_{31} = 0.1\%$ (-28.8 dB)	
Input fiber signal: 190mV (obtained by placing detector at focal point of lens #2).				

The data from coupler DC-1 indicates that, although coupling was achieved, it was not very efficient. The primary cause of this inefficiency was energy loss in the mixing rod portion of the coupler. When fiber #1 was under excitation by the laser, a large amount of light was seen to be escaping the coupler at the point where the other two fibers joined the mixing rod (Fig. 17). Two interrelated reasons for this loss are probable. The first, stemming from the fact that the quartz fibers and rod were unclad, was that the light rays could travel at large angles of incidence with respect to the the mixing rod axis. In other words, since the difference in refractive index is greater for this quartz-air situation than

it would be for a quartz-cladding situation, the critical angle for total internal reflection is smaller, as indicated by equation (10), page 12. Therefore, rays traveling at fairly large angles with respect to the coupler axis are allowed, and can consequently escape at the end of the mixing rod, where the walls are no longer uniform. The second reason for loss is the actual non-uniformity of the coupler's fabrication. This was clearly seen after the fabrication of a second directional coupler, DC-2. Fig. 18 is a photograph of the junction where the two output fibers join the mixing rod. The junction is obviously not as smooth as it was for coupler DC-1, and test results indicated much less coupling efficiency:

$$\text{Tap Ratios: } C_{12} = 0.1\% \text{ } (-32 \text{ dB}) \quad (62)$$

$$C_{13} = 0.02\% \text{ } (-37 \text{ dB}) \quad (63)$$

$$\text{Insertion Loss: } L_1 = -30.7 \text{ dB} \quad (64)$$

In an attempt to alleviate some of the loss problems with these couplers, it was thought that some sort of reflective coating on the ends of the mixing rod would help. Both couplers were coated (on each end) with type 8010-271-9751 silver spray paint and re-tested. Results in both cases were even less favorable than before, perhaps due to light absorption by the paint.

b) Tee Coupler (TC-1)

It should be mentioned that another coupler of this design was fabricated, although the results were poor. This coupler was of the tee variety, having two fibers drawn from each end of its solid quartz mixing rod (Fig. 20). Because this coupler,

TC-1, required fabrication techniques similar to the directional couplers, the coupling efficiency was negligible and no further discussion of its performance is necessary. It appears that, for this kind of design to be feasible, extremely delicate and difficult techniques are required for the actual pulling of the fibers. The better results stem from smooth and uniform joints where the two fibers meet at the end of the mixing rod.

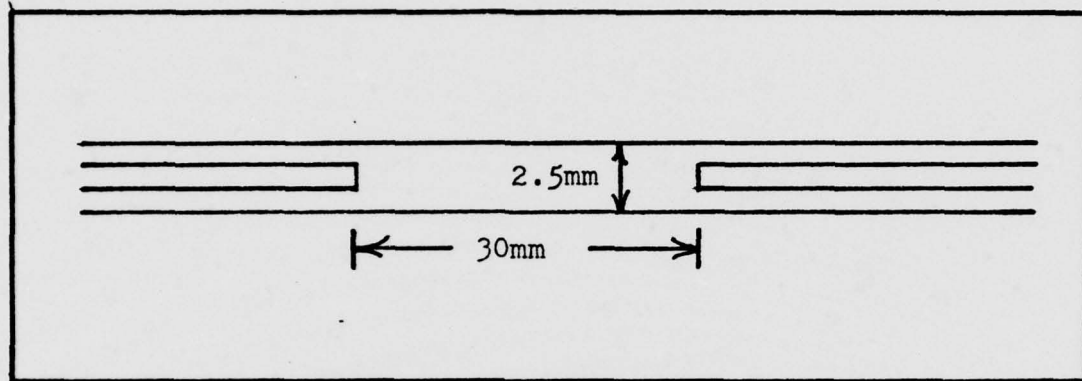


Fig. 20. Schematic of TC-1

c) Star Couplers (SC-1, SC-2, SC-3)

The next type of coupler fabricated and tested was of the radial, or star variety. The general design of the first three star couplers consisted of seven multimode fibers, a length of quartz tubing filled with a transparent cement, and a reflective surface on one end of the tubing (Fig. 21). The first two (SC-1 and SC-2) were prototypes put together using readily available materials, their purpose being to determine the feasibility of extensive design of this idea. The preliminary results of these models were promising, thus permitting the design procedure which follows.

The basic unit of the star coupler is the mixing rod, and therefore its dimensions must be determined from equation (32):

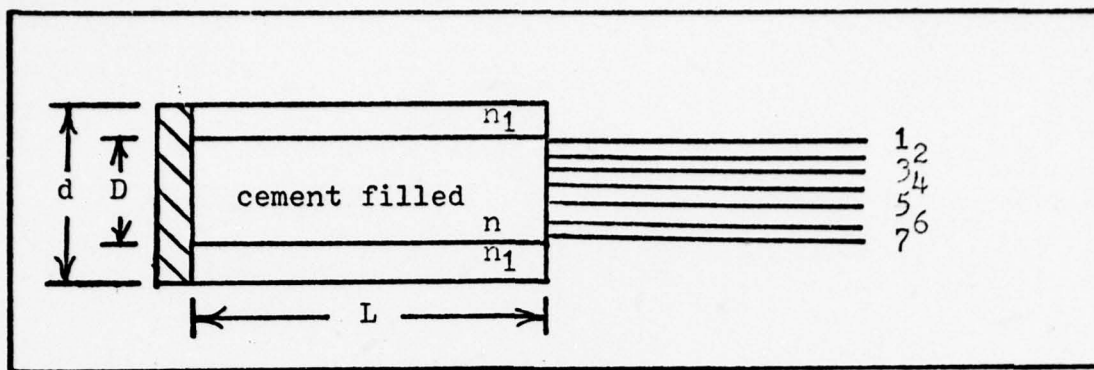


Fig. 21. General design of star coupler using cement-filled mixing rod

$$\frac{D}{L} = 2 \left[\frac{NA_f}{n^2 - (NA_f)^2} \right]^{\frac{1}{2}}, \quad (32)$$

where in this case,

D = inside diameter of the tube,

L = distance from the reflective surface to the fibers,

NA_f = numerical aperture of a single fiber,

n = index of refraction of cement.

The following materials were used:

- a) 7 fibers: DuPont PFX plastic, $NA_f = 0.53$, core radius = 0.18mm
- b) Mixing rod: quartz tubing, $n_1 = 1.5$, $D = 2\text{mm}$, $d = 3\text{mm}$
- c) Cement: Steven's Industries Adhesive and Sealing Compound
- d) Reflective surface: aluminum foil, 3mm x 3mm

As can be seen from the above list, the only unknown on the right-hand side of equation (32) is the index of the cement, n . This value was found by a method similar to that described on page 38. Here, a sample length of quartz tubing was filled with the cement in question and placed in the experimental set-up

such that one end of the tube was located at the focal point of lens #2. A white card was placed perpendicular to the axis of the tube at a distance $x = 10\text{mm}$ away from the end of the tube. When the laser was turned on, the radius, r , of the spot appearing on the card was measured (Fig. 22). Using equation

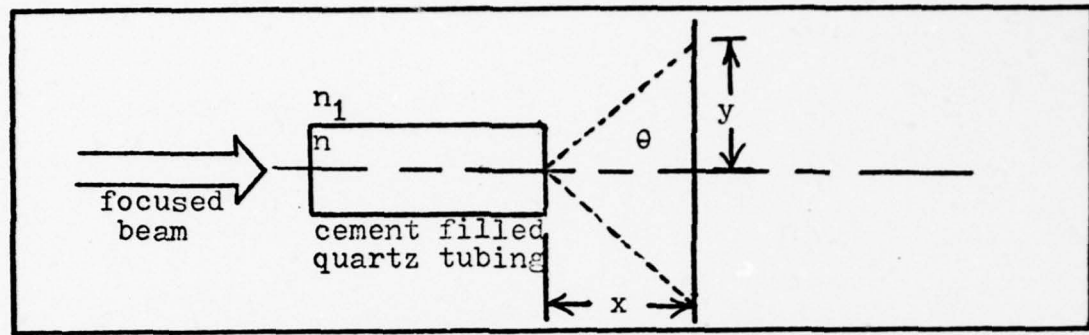


Fig. 22. Diagram of index measuring set-up (22) and relating it to the mixing rod (cement filled tube), the following equation is obtained:

$$NA_{\text{mix rod}} = (1)\sin\theta = [n^2 - n_1^2]^{\frac{1}{2}}, \quad (65)$$

where

$$\sin\theta = \sin\left[\tan^{-1}\left(\frac{r}{x}\right)\right]. \quad (66)$$

Solving for the unknown index,

$$n = \left\{ \left[\sin\left(\tan^{-1} \frac{r}{x}\right) \right]^2 + n_1^2 \right\}^{\frac{1}{2}}. \quad (67)$$

Now, with $x = 10\text{mm}$, $r = 6\text{mm}$ (measured), and $n_1 = 1.5$, the index of the cement is $n = 1.58$. Using equation (32), the dimensions of the mixing rod should be

$$\frac{D}{L} = 2 \left[\frac{0.53}{(1.58)^2 - (0.53)^2} \right]^{\frac{1}{2}} = 0.72. \quad (68)$$

With an inside diameter of $D = 2\text{mm}$, the length of the mixing

rod would be

$$L = \frac{2\text{mm}}{0.72} = 2.78\text{mm} \quad . \quad (69)$$

Assembly of SC-3 proceeded as follows:

- a) The quartz tubing was cut to a 10mm length and its ends were sanded perpendicular to the axis of the tube.
- b) The seven fibers were inserted in one end such that the distance from their ends to the opposite end of the tube was 3mm.
- c) The 3mm length was filled with the transparent cement and capped with the aluminum foil.
- d) The assembly was allowed to set for three hours; at the end of this time, some small bubbles began to appear in the cement. By pushing the fibers a bit farther into the tube, most of the bubbles disappeared.

The set-up for testing the coupling efficiency of SC-3 was essentially the same as that used for the Spectronics star coupler (page 34), with the exception of the second lens. Because of the coupler's location in relation to the detector, a longer focal length lens was needed, i.e., lens #2 was replaced by lens #3 ($F = 22\text{cm}$). The following test procedure was then used:

- a) The coupler was placed in the set-up such that the end of fiber #1 was located at the focal point of lens #3.
- b) The laser was turned on and observations of the coupler under excitation were made.
- c) The detector was placed approximately 1mm in front of each of the other fiber ends, in turn, and the

corresponding outputs were recorded.

- d) The above procedure was repeated six times, each time using a different fiber as the input fiber.

The data obtained is summarized in Table IV. It should be noted that in obtaining the transmission factor (T_*) and insertion loss (L_*), the input fiber signal was chosen so that the results would be independent of the fibers used, and would be strictly an indication of the performance of the coupler itself. This method corresponds to that prescribed by Ref 15:5, wherein the input reference is obtained by recording the output of a single fiber as it is excited by the laser.

Table IV
Data from Star Coupler SC-3

Input Fiber	Output Fiber	Output, mV (Peak-to-Peak)	T_*	L_*
1	2	0.60	.019 (-17.3 dB)	-11.65 dB
	3	0.22	.007 (-21.6 dB)	
	4	0.12	.004 (-23.9 dB)	
	5	0.36	.011 (-19.5 dB)	
	6	0.75	.023 (-16.3 dB)	
	7	0.14	.004 (-23.6 dB)	
2	1	0.24	.008 (-20.9 dB)	-14.56 dB
	3	0.12	.004 (-23.9 dB)	
	4	0.20	.006 (-22.0 dB)	
	5	0.16	.005 (-23.0 dB)	
	6	0.32	.010 (-20.0 dB)	
	7	0.08	.003 (-26.0 dB)	
3	1	0.28	.009 (-20.6 dB)	-13.23 dB
	2	0.16	.005 (-23.0 dB)	
	4	0.08	.003 (-26.0 dB)	
	5	0.40	.013 (-19.0 dB)	
	6	0.48	.015 (-18.2 dB)	
	7	0.12	.004 (-23.9 dB)	

(continued on next page)

Table IV
(continued)

Input Fiber	Output Fiber	Output, mV (Peak-to-Peak)	T*	L*
4	1	not measurable		
	2	0.12	.004 (-23.9 dB)	-17.27 dB
	3	0.08	.003 (-26.0 dB)	
	5	0.12	.004 (-23.9 dB)	
	6	0.14	.004 (-23.6 dB)	
	7	0.14	.004 (-23.6 dB)	
5	1	0.26	.008 (-20.9 dB)	-11.21 dB
	2	0.12	.004 (-23.9 dB)	
	3	0.20	.006 (-22.0 dB)	
	4	0.10	.003 (-25.1 dB)	
	6	1.50	.047 (-13.3 dB)	
	7	0.24	.008 (-20.9 dB)	
6	1	0.40	.013 (-19.0 dB)	-10.14 dB
	2	0.42	.013 (-18.8 dB)	
	3	0.70	.022 (-16.6 dB)	
	4	0.18	.006 (-22.5 dB)	
	5	1.20	.038 (-14.3 dB)	
	7	0.20	.006 (-22.0 dB)	
7	1	0.08	.003 (-26.0 dB)	-15.5 dB
	2	0.08	.003 (-26.0 dB)	
	3	0.08	.003 (-26.0 dB)	
	4	0.10	.003 (-25.1 dB)	
	5	0.36	.011 (-19.5 dB)	
	6	0.20	.006 (-22.0 dB)	
Input fiber signal: 32mV (obtained by recording the output of a single fiber when excited by the laser).				

As seen from Table IV, the coupling efficiency of SC-3 was satisfactory, but not exceptional. Observation of the coupler under excitation revealed significant loss coming from the mixing rod. Two primary sources of this loss were the reflecting surface at the end of the rod, and the inconsistencies of the cement inside the rod. The first was most likely due to the non-uniform surface of the aluminum foil, and could be reduced by using a more planar reflecting surface. The second, which included scattering of the light off of air bubbles in the

cement, could be eliminated by using a transparent adhesive which would prohibit the formation of bubbles. This bubble formation was observed to increase as the cement continued to harden, perhaps the result of air pushing through the tube, between the fibers. Several types of epoxy cements were tested in an attempt to obtain better results, but none hardened without the formation of air bubbles.

It should also be noted that the results varied, depending upon which fiber was used as the input fiber. Microscopic observation of the fibers revealed small variations in their outside diameter from one fiber to the next. If the light conducting cores also varied, this could be one reason for the inconsistency of the data. Another possibility lies in each fiber termination. The fibers were cut by scribing and breaking, thus allowing variation in the amount and angle of light entering and exiting the fibers.

Other losses to be considered are the packing fraction loss at the fiber-mixing rod boundary, the reflective losses at each interface, and the absorption loss introduced by the aluminum mirror.

An analysis of these losses will now be made, following the input signal from its entrance into the coupler to its exit from a single output fiber. Because of the method used in measuring the input reference signal, the value of 32mV input has allowed for the reflection loss at each end of the input fiber. Therefore, the first reduction of that value occurs at the cement interface. Using equation (42) the reflectivity at this interface, r_1 , is given by

$$r_1 = \left(\frac{n - 1}{n + 1} \right)^2 , \quad (70)$$

where $n = \frac{n_2}{n_1}$, n_1 = the index of air = 1, n_2 = the index of the cement = 1.58. Substituting these values gives

$$r_1 = 0.05 . \quad (71)$$

The next surface encountered by the signal is that of the aluminum foil at the end of the mixing rod. The reflectivity of this surface, r_2 , was measured spectrographically at 6328Å to be

$$r_2 = 0.70 . \quad (72)$$

After traveling back through the mixing rod, the signal experiences the packing fraction loss given by equation (43):

$$L_{p.f.} = \frac{A_f}{A_r} . \quad (43)$$

For fiber core radii of 0.18mm and the mixing rod inside radius of 1.0mm, this packing fraction becomes

$$L_{p.f.} = 0.23 . \quad (73)$$

When considering the output of one individual fiber, the added reduction of the signal strength by $\frac{1}{7} = 0.143$ must also be included. Finally, the reflective losses at each end of the output fiber are needed. The first interface is a cement/fiber one, and again using equation (42), the reflectivity, r_3 , of this boundary is

$$r_3 = 0.001 , \quad (74)$$

where in this case, n_1 = the index of cement = 1.58 and n_2 = the index of the fiber = 1.49. The second interface is a fiber/air boundary, which gives a reflectivity, r_4 , of

$$r_4 = 0.04 \quad , \quad (75)$$

where n_1 = the index of the fiber = 1.49 and n_2 = the index air = 1. Combining the above losses as they degrade the original input V_{in} reveals a theoretical output, V_{out} , of

$$V_{out} = V_{in}(1 - r_1)(r_2)(L_{p.f.})(0.143)(1 - r_3)(1 - r_4). \quad (76)$$

Substituting the values obtained above,

$$V_{out} = 32mV(.95)(.70)(.23)(.143)(.999)(.96) = .671mV. \quad (77)$$

This gives a T_* of 0.021, which is a signal reduction of -16.78 dB. As a comparison to experimental results, the average value of T_* calculated from Table IV is

$$T_*(ave) = 0.009 = -20.5 \text{ dB} \quad . \quad (78)$$

The difference in the two values can be attributed to the lossy mixing rod described previously.

d) Star Coupler (SC-4)

This design for a star coupler employs a solid quartz mixing rod which has been coated on one end and on its sides with a reflective material. The input/output fibers are butted against the opposite end and the unit is held together with heat-shrink tubing (Fig. 23). The following materials were used in its fabrication:

- a) 7 fibers: DuPont PFX plastic, $NA_f = 0.18mm$

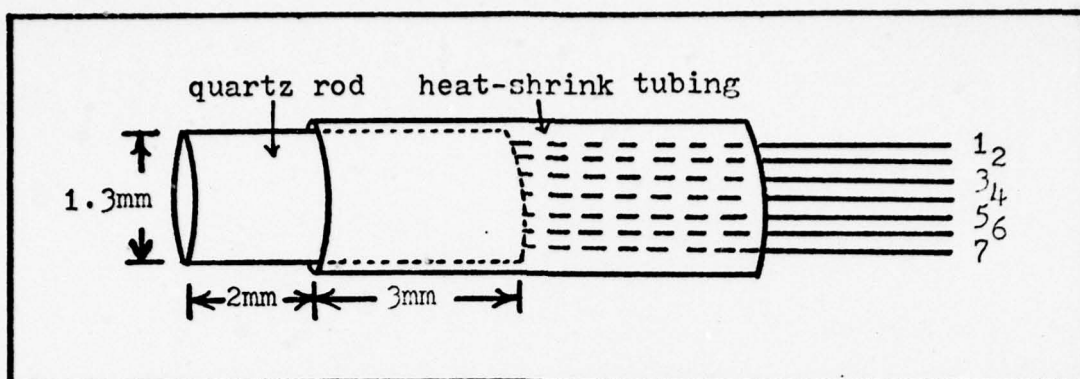


Fig. 23. Diagram of star coupler with solid mixing rod

- b) Mixing rod: solid quartz rod, $D = 1.3\text{mm}$, $L = 5\text{mm}$,
 $n = 1.5$
- c) Reflective coating: silvering solution (Ref 13:407-409)
- d) Heat-shrink tubing: inner diameter = 1.6mm , length
= 10mm

Design parameters were again obtained from equation (32), which gives a diameter-to-length ratio using the materials above of

$$\frac{D}{L} = \frac{2(0.53)}{\left[(1.5)^2 - (0.53)^2\right]^{\frac{1}{2}}} = 0.76 \quad (79)$$

For a diameter of 1.3mm , the resulting minimum length for the mixing rod would be

$$L = \frac{1.3\text{mm}}{.76} = 1.71\text{mm} \quad (80)$$

Due to the glass working problems of handling such a small device, the length was chosen to be a manageable 5mm . After the rod was cut to length, its ends were fire-polished to make them optically transparent (Fig. 24).



Fig. 24. Microscopic photograph of mixing rod for SC-4

Actual fabrication began by inserting the quartz rod 3mm into the heat-shrink tubing, thus keeping 2mm of the rod exposed. The seven fibers were then inserted in the other end of the tubing until they contacted the mixing rod. The tubing was then heated, securing the fibers and rod into one unit. The exposed section of quartz rod was then dipped into the silvering solution for twenty minutes, such that a uniform reflective coating was deposited on the quartz. The silvering solution had been made earlier using the following materials:

- a) 2.38oz cane sugar
- b) 3.0ml nitric acid
- c) 500ml distilled water
- d) 5.0gm silver nitrate
- e) 2.5gm potassium hydroxide
- f) 15.0ml ammonium hydroxide

Preparation and mixing of these chemicals is described in Ref 13:408.

The following procedure was used in evaluating the efficiency of SC-4:

- a) Using the same set-up as that for SC-3, the coupler was placed such that the end of fiber #1 was located at the focal point of lens #3.
- b) The laser was turned on and observations of the coupler under excitation were made.
- c) The detector was placed approximately 1mm in front of each of the other fiber ends, in turn, and the corresponding outputs were recorded.
- d) The above procedure was repeated six times, each time using a different fiber as the input fiber.

The data obtained is summarized in Table V. The input fiber signal was measured as described on page .

Table V
Data from Star Coupler SC-4

Input Fiber	Output Fiber	Output, mV (Peak-to-Peak)	T*	L*
1	2	0.16	.005 (-23.0 dB)	-16.13 dB
	3	0.08	.003 (-26.0 dB)	
	4	0.24	.008 (-21.2 dB)	
	5	0.20	.006 (-22.0 dB)	
	6	0.04	.001 (-29.0 dB)	
	7	0.06	.002 (-27.0 dB)	
2	1	0.16	.005 (-23.0 dB)	-16.9 dB
	3	0.08	.003 (-26.0 dB)	
	4	0.20	.006 (-22.0 dB)	
	5	0.10	.003 (-25.1 dB)	
	6	0.08	.003 (-26.0 dB)	
	7	0.04	.001 (-29.0 dB)	

(continued on next page)

Table V
(continued)

Input Fiber	Output Fiber	Output, mV (Peak-to-Peak)	T*	L*
3	1	0.08	.003 (-26.0 dB)	-17.3 dB
	2	0.08	.003 (-26.0 dB)	
	4	0.20	.006 (-22.0 dB)	
	5	0.12	.004 (-23.9 dB)	
	6	0.08	.003 (-26.0 dB)	
	7	0.04	.001 (-29.0 dB)	
4	1	0.24	.008 (-20.9 dB)	-15.1 dB
	2	0.20	.006 (-22.0 dB)	
	3	0.12	.004 (-23.9 dB)	
	5	0.20	.006 (-22.0 dB)	
	6	0.14	.004 (-23.6 dB)	
	7	0.08	.003 (-26.0 dB)	
5	1	0.10	.003 (-25.1 dB)	-19.7 dB
	2	0.02	.001 (-32.0 dB)	
	3	0.04	.001 (-29.0 dB)	
	4	0.16	.005 (-23.0 dB)	
	6	0.02	.001 (-32.0 dB)	
	7	not measurable	—	
6	1	not measurable	—	-26.0 dB
	2	0.02	.001 (-32.0 dB)	
	3	not measurable	—	
	4	0.06	.002 (-27.3 dB)	
	5	not measurable	—	
	7	not measurable	—	
7	1	0.02	.001 (-32.0 dB)	-25.1 dB
	2	0.02	.001 (-32.0 dB)	
	3	0.02	.001 (-32.0 dB)	
	4	0.04	.001 (-29.0 dB)	
	5	not measurable	—	
	6	not measurable	—	
Input fiber signal: 32mV (obtained by recording the output of a single fiber when excited by the laser).				

Table V indicates that for SC-4, coupling was achieved, although it was not very efficient. When observing the coupler under excitation, it was noted that some light was escaping the mixing rod, from both the silvered surface and the input side of the rod. The former observation indicated that

the silvering process did not cover the quartz rod uniformly, while the latter was a reflection off the fiber/mixing rod interface.

A loss analysis similar to that involving SC-3 can now be made for SC-4, again following the input signal as it traverses the coupler. The first interface encountered by the signal as it leaves the input fiber is that of the quartz rod. Using equation (42) with $n = \frac{n_2}{n_1}$, $n_1 =$ the index of air = 1, and $n_2 =$ the index of the rod = 1.5, the reflectivity, r_1 , at this surface is

$$r_1 = \left(\frac{n - 1}{n + 1} \right)^2 = 0.04 \quad . \quad (81)$$

The signal then encounters the silvered end of the mixing rod, which has a reflectivity at 6328Å, r_2 , of (Ref 17:568)

$$r_2 = 0.95 \quad . \quad (82)$$

Next, after traveling back through the rod, the packing fraction loss given by equation (43) is then considered. Since the quartz rod has a radius of 0.65mm and the fibers have core radii of 0.18mm, the packing fraction is then

$$L_{p.f.} = 0.54 \quad . \quad (83)$$

Now, because the output of a single fiber is desired, another reduction in the signal by $\frac{1}{7} = 0.143$ must be included. The last two losses occur at the ends of the output fiber. These are reflective losses and equation (42) applies. The first of these is the quartz/fiber boundary with $n_1 = 1.5$ and $n_2 = 1.49$ which, because of the similarity in index, gives a negligible

loss. The second boundary is the fiber/air one, where $n_1 = 1.49$ and $n_2 = 1.0$. Substitution into equation (42) gives a reflectivity, r_3 , of

$$r_3 = 0.04 \quad . \quad (84)$$

Combining the above losses with the input, V_{in} , yields an output value, V_{out} , of

$$V_{out} = V_{in}(1 - r_1)(r_2)(L_{p.f.})(0.143)(1 - r_3). \quad (85)$$

Substituting the values obtained above,

$$V_{out} = 32\text{mV} (.96)(.95)(.54)(.143)(.96) = 2.16\text{mV}. \quad (86)$$

This output gives a T_* of 0.068, which is a signal reduction of -11.71 dB. As a comparison to experimental results, the average value of T_* calculated from Table V is

$$T_*(\text{ave}) = 0.003 = -25.2 \text{ dB} \quad . \quad (87)$$

Other than the observed light losses mentioned earlier, the primary reason for such a large difference between predicted and actual performance may lie in the fiber/mixing rod interface. It can be seen from the photograph of the rod (Fig. 24) that the ends are slightly rounded (most likely due to fire polishing). This surface shape could cause much of the light from the fibers near the outside edge of the rod to be reflected off at an angle, thus significantly reducing the coupler's effectiveness. In addition, the ends of the fibers were not perfectly flat, a factor which would also effect the signal's transfer from the input fiber to the mixing rod. In order for

the design to be feasible, then, improved techniques of cutting and polishing are required for both the fibers and the mixing rod.

e) Star Couplers (SC-5, SC-6)

The next design investigated for this experiment was a seven port star coupler fabricated by thermally fusing the fibers to themselves, forming a mixing rod (Fig. 25). Due to

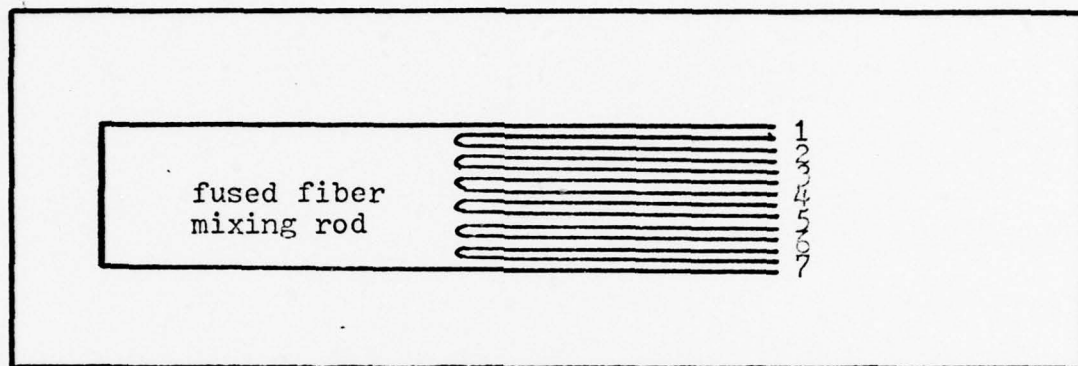


Fig. 25. Schematic of fused fiber star coupler

time constraints and available materials, fabrication was done on a purely qualitative basis, employing no specific design criteria. However, the mixing rod design equation (22) could be used, defining the fiber/mixing rod interface as that point where the fibers are no longer individuals, but fused into a solid rod (Fig. 25).

The equipment used in fabrication was the following:

- a) 7 fibers (SC-5): ITT PS-08-10
- b) 7 fibers (SC-6): Corning glass
- c) 2 glass cylinders, the inside diameters of which approximately matched the cross-sectional diameter of seven fibers. The length of each cylinder was 4cm.

- d) Polyurethane epoxy remover: Spec. MIL-R-81294A
- e) Oxygen fed torch

The procedure used in fabrication was the following:

- a) The plastic coating on the ITT fibers was stripped off after letting them soak in the epoxy remover for a period of ten minutes. Since the mixing rod in this device requires that the light-carrying fiber cores be in contact, the thin cladding on each fiber was also removed. Since the cladding was plastic and the core was glass, this was done by burning. Although this method seemed to make the fibers more brittle, other attempts using chemical strippers were unsuccessful. Removal of the cladding on the Corning fibers was also accomplished by burning. Both sets of fibers were then cleaned using methanol and distilled water.
- b) Each set of seven fibers was then inserted into separate glass cylinders in preparation for fusion. Preliminary tests which consisted of holding the fibers directly over the torch indicated that the fibers were too thin for this method of fusing. Therefore, by placing the fibers inside the glass tubing, the whole unit could then be held in the flame, the individual fibers being protected by the sheath of glass.
- c) Each unit of seven fibers surrounded by the glass tubing was then held in the torch flame until the fibers were observed to melt into each other. A

microscopic photograph of each mixing rod was taken and can be seen in Fig. 26 and Fig. 27.



Fig. 26. Photograph of SC-5: ITT fibers



Fig. 27. Photograph of SC-6: Corning fibers

Qualitative testing of both couplers was done by placing them in the experimental set-up and focusing the laser beam at the end of the mixing rod. Observation of the individual fibers' ends revealed very little or no transmission of the light. The couplers were turned around and the beam was focused on each end of the fibers, in turn. Observation of the mixing rod indicated that some of the fibers allowed the light to reach the end of the rod, while others appeared to have broken off near the front of the rod. This most likely occurred during

the heating process. Another problem encountered during heating was the deformation by melting of the rod after the fibers had been fused. Since the rod was then not perfectly straight, light entering the rod would not be totally contained in it, but rather escape at the bends. Because of the poor observations made on these two fusion attempts, no further development of them into star couplers was made.

ITT Fused Star Coupler Evaluation

The final coupler tested employed a set of seven fibers which had been thermally fused for a given length by ITT. The design is similar to that attempted in the previous section except that the fiber cores had been heated directly (no glass tubing was used) by a small, hydrogen fed torch. When placed in the experimental set-up, a silver coated mirror was placed adjacent to the end of the fused section, making a crude star coupler (Fig. 28). The fibers used were ITT PS-08-10.

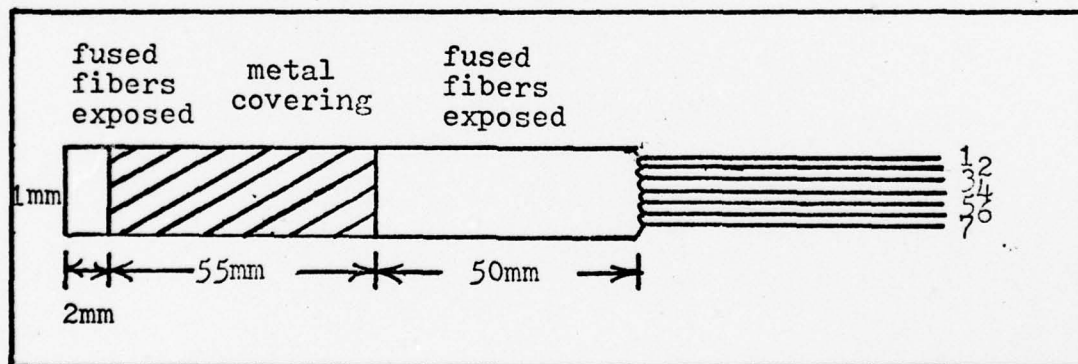


Fig. 28. Star coupler made from ITT fused fibers

The procedure used for coupling efficiency evaluation was as follows:

- a) The coupler was placed in the experimental set-up

such that the end of fiber #1 was at the focal point of lens #3.

- b) The laser was turned on and observations of the coupler under excitation were made.
- c) The detector was placed approximately 1mm in front of each of the other fibers' ends, in turn, and the corresponding outputs were recorded.
- d) The above procedure was repeated six times, each time using a different fiber as the input fiber.
- e) The coupler was removed from the set-up and replaced by a single ITT PS-08-10 fiber such that one end was at the focal point of lens #3.
- f) With the laser on, the output from the other end of the fiber was measured, thus providing an input reference signal from which T_* and L_* could be calculated.

Results of the evaluation are summarized in Table VI.

Table VI
Data from ITT Fused Fiber Star Coupler

Input Fiber	Output Fiber	Output, mV (Peak-to-Peak)	T_*	L_*
1	2	0.20	.013 (-19.0 dB)	-13.23 dB
	3	0.12	.008 (-20.9 dB)	
	4	0.12	.008 (-20.9 dB)	
	5	0.10	.006 (-22.0 dB)	
	6	0.12	.008 (-20.9 dB)	
	7	0.10	.006 (-22.0 dB)	

(continued on next page)

Table VI
(continued)

Input Fiber	Output Fiber	Output, mV (Peak-to-Peak)	T*	L*
2	1	0.18	.011 (-19.5 dB)	-10.9 dB
	3	0.22	.014 (-18.6 dB)	
	4	0.26	.016 (-17.9 dB)	
	5	0.24	.015 (-18.2 dB)	
	6	0.20	.013 (-19.0 dB)	
	7	0.20	.013 (-19.0 dB)	
3	1	0.08	.005 (-23.0 dB)	-13.59 dB
	2	0.10	.006 (-22.0 dB)	
	4	0.14	.009 (-20.6 dB)	
	5	0.12	.008 (-20.9 dB)	
	6	0.14	.009 (-20.6 dB)	
	7	0.12	.008 (-20.9 dB)	
4	1	0.08	.005 (-23.0 dB)	-13.72 dB
	2	0.12	.008 (-20.9 dB)	
	3	0.10	.006 (-22.0 dB)	
	5	0.10	.006 (-22.0 dB)	
	6	0.14	.009 (-20.6 dB)	
	7	0.14	.009 (-20.6 dB)	
5	1	0.12	.008 (-20.9 dB)	-12.90 dB
	2	0.12	.008 (-20.9 dB)	
	3	0.14	.009 (-20.6 dB)	
	4	0.12	.008 (-20.9 dB)	
	6	0.12	.008 (-20.9 dB)	
	7	0.20	.013 (-19.0 dB)	
6	1	0.18	.011 (-19.5 dB)	-11.55 dB
	2	0.20	.013 (-19.0 dB)	
	3	0.16	.010 (-20.0 dB)	
	4	0.24	.015 (-18.2 dB)	
	5	0.18	.011 (-19.5 dB)	
	7	0.16	.010 (-20.0 dB)	
7	1	0.16	.010 (-20.0 dB)	-11.47 dB
	2	0.24	.015 (-18.2 dB)	
	3	0.20	.013 (-19.0 dB)	
	4	0.20	.013 (-19.0 dB)	
	5	0.18	.011 (-19.5 dB)	
	6	0.16	.010 (-20.0 dB)	
Input signal: 16mV (obtained by recording the out- put of a single fiber when excited by the laser).				

Table VI shows that both the individual transmission factors (T* values) and the insertion losses (L* values) were generally

better than previous designs. Note also that the outputs were fairly uniform for a given input fiber. This indicates that by proper fusion of the fibers, a better mixing rod (in terms of uniform distribution of the signal) is obtained. Observation of the coupler under excitation revealed some light loss at the mixing rod/mirror interface. Improved transmission factors might be obtained if the entire mixing rod was reflectively coated.

A loss analysis for this coupler can be made, similar to that done for SC-3 and SC-4. However, because of the fused nature of this device, the only reflective interfaces to be considered are the mirrored surface and the output fiber/air boundary. In addition, the packing fraction loss is approximately 1.0 (0.0 dB), since the combined cross-sectional areas of the fibers form the cross-sectional area of the mixing rod. Therefore, taking the reflectivity of the mirror to be 0.95, the index of the fiber cores to be $n = 1.46$, and remembering the $\frac{1}{7} = 0.143$ reduction at the mixing rod/fiber interface, the output expected from one fiber given an input of 16mV is

$$V_{\text{out}} = (16\text{mV})(.95)(.143)(.96) = 2.087\text{mV} \quad . \quad (88)$$

This output gives a T_* of 0.130, which is a signal reduction of -8.85 dB. As a comparison to experimental results, the average value of T_* calculated from Table VI is

$$T_* = 0.010 = -20.0 \text{ dB} \quad . \quad (89)$$

The difference in the two values can be attributed to the losses observed at the mirror.

SUMMARY, CONCLUSION, AND RECOMMENDATION

Discussions found in the foregoing sections have dealt with the design and evaluation of couplers for a fiber optic data transmission system. Following a brief summary of theoretical approach to waveguide energy propagation and a look at the design parameters involving fiber optic couplers, experimental concentration was centered on single strand, step index, multimode fibers. Experience in working with coupler operation and efficiency measurement was gained by the evaluation of two available couplers, the Hughes Laboratories single fiber tee coupler and the Spectronics, Inc. fiber bundle star coupler.

Fabrication of devices specifically for this project began with two directional couplers and one tee coupler, all formed by employing glass pulling techniques in conjunction with solid quartz mixing rods. Results of this effort were not substantial.

Because of the inherent advantages of a single star coupler over several tee couplers in a short range data bus system (centralized location and less reflective losses at each terminal), the main emphasis was then shifted toward various star coupler designs. The primary element for design consideration was the mixing rod, and this project dealt with three different types: a transparent cement-filled tube, a solid quartz rod, and fiber fusion.

The two basic evaluation parameters used in comparing the above-mentioned designs are the transmission factor (T_*), defined

by equation (58), and the insertion loss (L_*), defined by equation (59). Table VII provides a summary of these two parameters for each of the three designs, listing both the predicted value and the experimentally measured value. The latter is the average of that which was actually measured for each device.

Table VII
Comparison between Star Couplers

Coupler	T_* predicted	$T_*(\text{ave})$ measured	L_* predicted	$L_*(\text{ave})$ measured
SC-3	.021 (-16.78 dB)	.009 (-20.5 dB)	-9.00 dB	-12.83 dB
SC-4	.068 (-11.71 dB)	.003 (-25.2 dB)	-3.93 dB	-18.01 dB
ITT fused fiber	.130 (-8.85 dB)	.010 (-20.0 dB)	-1.06 dB	-12.35 dB

Looking only at the experimentally measured results, Table VII shows that SC-3 and the fused fiber coupler had similar efficiencies, while the performance of SC-4 was not as good. It is interesting to note, however, that the predicted values indicate a different situation. These figures indicate that SC-4 should perform better than SC-3. The reason for this discrepancy probably lies in the fabrication techniques used in coupler construction. As discussed in the experimental section, the fiber/mixing rod interface is critical in the production of reflective losses. Whereas SC-3 was made such that the fibers contacted an initially liquid cement, the SC-4 fibers were merely held against a solid quartz rod by way of heat-shrink tubing. Because the fiber ends and the end of the

mixing rod were not perfectly flat at their junction, the latter design allowed more reflective losses. Perhaps an index matching cement sealing the fibers and mixing rod to each other would have improved the performance of SC-4.

The predicted values for the fused fiber star coupler indicate that a very good coupling efficiency is possible. In fact, primarily because of the elimination of reflective and packing fraction losses at the fiber/mixing rod interface, the fused fiber design could approach an optimum coupling efficiency. The main source of internal loss for this case lies in the mirror surface absorption and, for the experiment described on page 61, the primary external loss of energy occurred at the junction of the mixing rod and mirror. A better method of fabrication would involve coating the mixing rod with a highly reflective surface, thus eliminating the majority of these losses.

Results of this project, then, enable the recommendation of a single-strand, multimode fiber star coupler whose mixing rod is formed by fusion of the individual fibers and which is coated with a substance that provides maximum reflectivity in the region of the signal's wavelength.

Bibliography

1. Kapany, N. S., and J. J. Burke. Optical Waveguides. New York: Academic Press, 1972.
2. Marcuse, D. Light Transmission Optics. New York: VanNostrand Reinhold Co., 1972.
3. Born, M., and E. Wolf. Principles of Optics. Oxford: Pergamon Press, 1975.
4. AFAL-TR-74-314. Optical Couplers. Texas: Spectronics, Inc., December 1975.
5. Barnoski, M. K. Fundamentals of Optical Fiber Communications. New York: Academic Press, Inc., 1976.
6. Barnoski, M. K., and H. R. Friedrich. "Fabrication of an Access Coupler with Single-Strand Multimode Fiber Waveguides." Applied Optics, 15:2629-2630 (November 1976).
7. -----. Optical Fiber Components and Accessories. New York: Math Associates, 1977.
8. -----. "Guided Optical Communications." Proceedings of Society of Photo-Optical Instrumentation Engineers. California: August 1975.
9. -----. "Mode Scrambler for Optical Fibers." Applied Optics, pg. 1045 (April 1977).
10. Marcuse, D. Intergrated Optics. New York: IEEE Press, 1973.
11. -----. "Optical Communication." Electronics, 49:81-104 (August 1976).
12. Takahashi, K., and S. Nonaka. "Optical Directional Coupler." Optical Fiber Transmission, II:WA5-1 (February 1977).
13. Brown, E. B. Optical Instruments. New York: Chemical Publishing Co., 1954.
14. Kawasaki, B. S., and K. O. Hill. "Low-loss Access Coupler for Multimode Optical Fiber Distribution Networks." Applied Optics, 16:1794-1795 (September 1977).
15. -----. Statement of Work, Single Fiber Star Coupler Development. Naval Ocean System Center (1977).

16. Ozeki, T., and B. S. Kawasaki. "Optical Directional Coupler using Tapered Sections in Multimode Fibers." Applied Physics Letters, 28:528-529 (May 1976).
17. -----. Optical Properties and Electronic Structure of Metals and Alloys, edited by F. Abeles. New York: North-Holland Publishing Co., 1966.
18. -----. Electro-Optical Systems Design, pg. 31 (October 1976).
19. -----. "Communications." Spectrum, 14:32-41 (February 1977).

Appendix

DETECTOR LINEARITY MEASUREMENT

In order to determine the variation of voltage detected with the amount of power reaching the detector, the following equipment was used:

- a) HeNe laser: Spectra Physics (power measured to be 1.4mW)
- b) Chopper: Bulova 150Hz
- c) Neutral density filters: Optics Technology, Inc.
- d) Detector: HP p-i-n photodiode, 5082-4205
- e) Oscilloscope: Tektronix type 555

The set-up used is indicated in Fig. 29. Various combinations

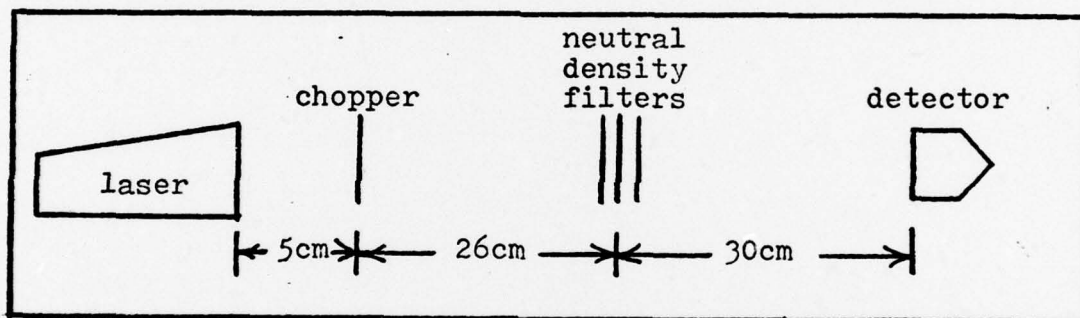


Fig. 29. Set-up for detector linearity measurement

of the neutral density filters were placed in the beam path and the output from the detector was read from the oscilloscope. The data obtained is recorded in Table VIII. Since the neutral density filters are such that #1 allows 10% transmission of power, #2 allows 1% transmission of power, #3 allows 0.1% transmission of power, and #4 allows 0.01% transmission of power, the graph in Fig. 30 of measured voltage versus percent of power transmission was drawn. This plot indicates that the voltage measured by the detector, V_m , is linear with the power,

Table VIII
Detector Output for Neutral Density Filters

Neutral Density	Output, mV (Peak-to-Peak)
1	5600.0
2	440.0
2 + 1	47.0
4	4.0

P, it receives, i.e.

$$V_m = KP, \quad (90)$$

where K is some constant of proportionality. Such a relation allows the valid use of equations (45) and (59), i.e., dB values can be calculated directly from the detector output as power ratios:

$$\text{dB} \Big|_{\text{power}} = 10 \log \left(\frac{P_1}{P_2} \right) \quad (91)$$

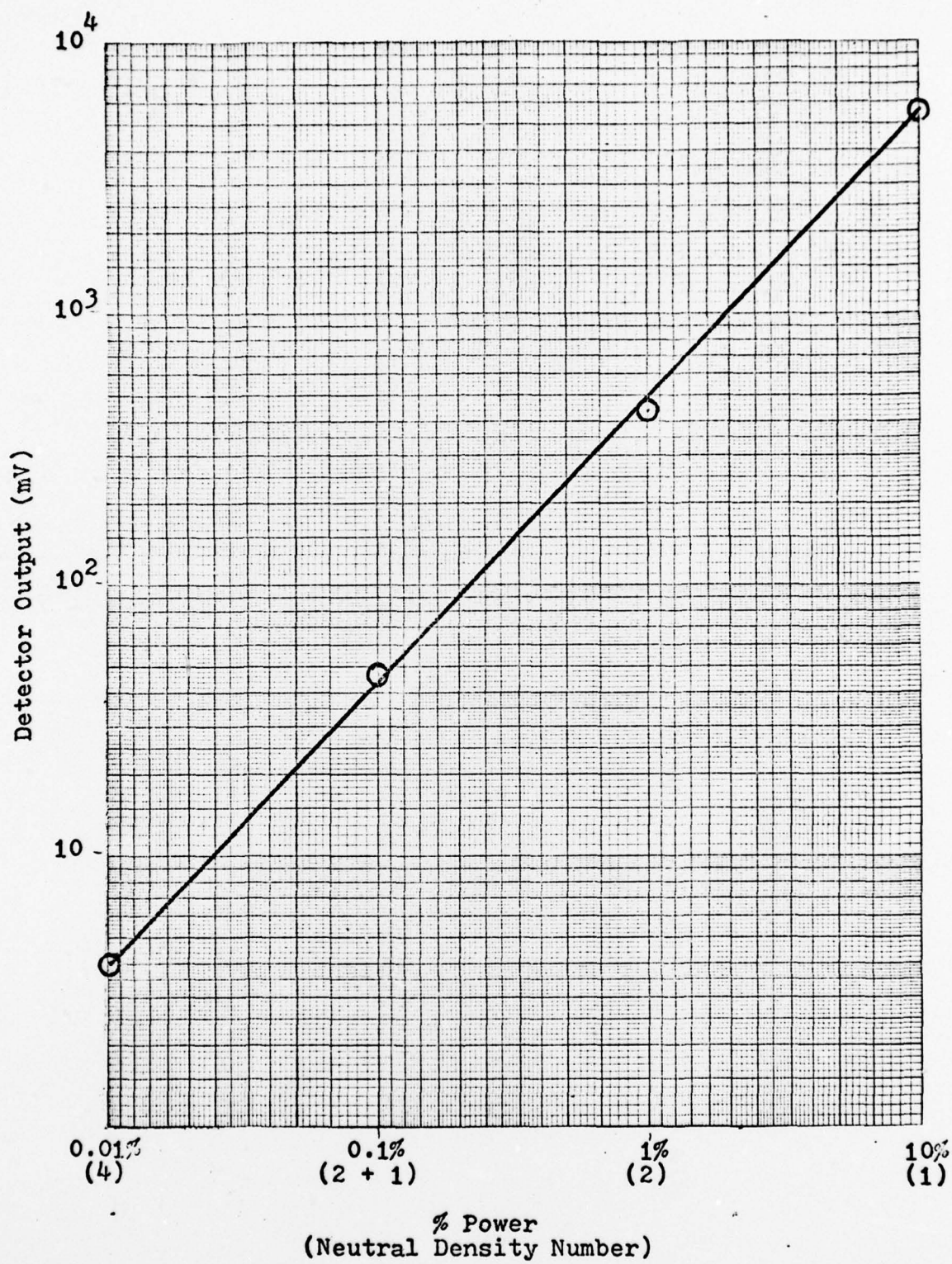


Fig. 30. Plot of detector voltage vs. power received

VITA

Michael C. Ogan was born on 7 January 1954 in Wichita Falls, Texas. He graduated from Radford High School in Honolulu, Hawaii in 1972 and attended the University of Hawaii, from which he received a Bachelor of Science degree in Electrical Engineering on 15 May 1976. Upon graduation, he received a commission in the USAF through the ROTC program. He was called to active duty in August, 1976, his first assignment being a student in the Electro-optics graduate program at the Air Force Institute of Technology.

Permanent address: 1709 Piikea St.

Honolulu, Hawaii 96818

UNCLASSIFIED

SECURITY CLASSIFICATION OF THIS PAGE (When Data Entered)

REPORT DOCUMENTATION PAGE		READ INSTRUCTIONS BEFORE COMPLETING FORM
1. REPORT NUMBER GEO/PH/77-2 ✓	2. GOVT ACCESSION NO.	3. RECIPIENT'S CATALOG NUMBER
4. TITLE (and Subtitle) DESIGN AND EVALUATION OF COUPLERS FOR A MULTIMODE SINGLE FIBER OPTICAL DATA BUS		5. TYPE OF REPORT & PERIOD COVERED MS Thesis
7. AUTHOR(s)		6. PERFORMING ORG. REPORT NUMBER
9. PERFORMING ORGANIZATION NAME AND ADDRESS Air Force Institute of Technology (AFIT- Wright-Patterson AFB, Ohio 45433 ✓EN)		8. CONTRACT OR GRANT NUMBER(s)
11. CONTROLLING OFFICE NAME AND ADDRESS AFAL-DHO Air Force Avionics Laboratory Wright-Patterson AFB, Ohio 45433		10. PROGRAM ELEMENT, PROJECT, TASK AREA & WORK UNIT NUMBERS
14. MONITORING AGENCY NAME & ADDRESS (if different from Controlling Office)		12. REPORT DATE October, 1977
		13. NUMBER OF PAGES 75
		15. SECURITY CLASS. (of this report) Unclassified
		15a. DECLASSIFICATION/DOWNGRADING SCHEDULE
16. DISTRIBUTION STATEMENT (of this Report) Approved for public release; distribution unlimited		
17. DISTRIBUTION STATEMENT (of the abstract entered in Block 20, if different from Report)		
18. SUPPLEMENTARY NOTES Approved for public release; IAW AFR 190-17 JERRAL F. GUESS, Captain, USAF Director of Information		
19. KEY WORDS (Continue on reverse side if necessary and identify by block number) Fiber Optics Fiber Optic Coupler Star Coupler Single-strand, Multimode Fiber		
20. ABSTRACT (Continue on reverse side if necessary and identify by block number) The fiber optic couplers designed and evaluated in this thesis are intended primarily for use in aircraft avionics systems, and consist of single strand, multimode fibers with step index profiles. Types of couplers considered are the directional, tee, and star couplers, with emphasis on the latter. Several designs are fabricated and tested, including three kinds of star couplers. The first employed a mixing rod of transparent cement and yielded an average transmission factor of 0.009 (-20.5 dB), with an		

DD FORM 1473

EDITION OF 1 NOV 65 IS OBSOLETE

UNCLASSIFIED

SECURITY CLASSIFICATION OF THIS PAGE (When Data Entered)

UNCLASSIFIED

SECURITY CLASSIFICATION OF THIS PAGE(When Data Entered)

average insertion loss of -12.83 dB. The second was formed with a solid quartz mixing rod, producing an average transmission factor of 0.003 (-25.2 dB) and an average insertion loss of -18.01 dB. The third star coupler's mixing rod was made by fusing the individual fibers, resulting in an average transmission factor of 0.01 (-20.0 dB) and an average insertion loss of -12.35 dB. After theoretical and experimental comparison between performance efficiencies, the third coupler is recommended as an optimum design for a fiber optic data bus system.

UNCLASSIFIED

SECURITY CLASSIFICATION OF THIS PAGE(When Data Entered)